1,3,5-Triamino-1,3,5-trideoxy-*cis*-inositol, a Ligand with a Remarkable Versatility for Metal Ions. 5. Complex Formation with Magnesium(II), Calcium(II), Strontium(II), Barium(II), and Cadmium(II)

Kaspar Hegetschweiler,*[1a] Robert D. Hancock,[1b] Michele Ghisletta,[1a] Thomas Kradolfer,[1a] Volker Gramlich,[1c] and Helmut W. Schmalle[1d]

Laboratorium für Anorganische Chemie, ETH-Zentrum, CH-8092 Zürich, Switzerland, Centre for Molecular Design, Department of Chemistry, University of the Witwatersrand, WITS 2050, Johannesburg, South Africa, Institut für Kristallographie und Petrographie, ETH Zentrum, CH-8092 Zürich, Switzerland, and Anorganisch-Chemisches Institut der Universität Zürich, Winterthurerstrasse 190, CH-8057 Zürich, Switzerland

Received April 15, 1993[⊕]

Solid compounds containing the complexes $[Cd(taci)_2]^{2+}$, $[Mg(taci)_2]^{2+}$, $[Ca(taci)_2(H_2O)_2]^{2+}$, $[Sr(taci)_2(H_2O)_3]^{2+}$, and $[Ba(taci)_2(H_2O)_3]^{2+}$ (taci = 1,3,5-triamino-1,3,5-trideoxy-*cis*-inositol) have been prepared by combining aqueous solutions of taci and of corresponding MX_2 salts (X = NO_3, Br, ClO_4). X-ray data: taci·$2H_2O$, $C_6H_{19}N_3O_5$, monoclinic, space group $P2_1/n$, a = 12.002(6) Å, b = 5.506(3) Å, c = 15.588(8) Å, β = 97.30(3)°, Z = 4; $[Cd(taci)_2](NO_3)_2·2H_2O$, $C_{12}H_{34}CdN_8O_{14}$, monoclinic, space group $P2_1/c$, a = 7.110(2) Å, b = 8.717(3) Å, c = 18.781(7) Å, β = 100.54(3)°, Z = 2; $[Mg(taci)_2](ClO_4)_{1.5}(OH)_{0.5}·5.25H_2O$, $C_{12}H_{41}Cl_{1.5}MgN_6O_{17.75}$, triclinic, space group $P\bar{1}$, a = 11.314(3) Å, b = 11.448(3) Å, c = 12.134(3) Å, α = 111.57(2)°, β = 103.16(2)°, γ = 105.32(2)°, Z = 2; $[Ca(taci)_2(H_2O)_2]Br_2·6H_2O$, $C_{12}H_{46}Br_2CaN_6O_{14}$, triclinic, space group $P\bar{1}$, a = 10.879(2) Å, b = 12.061(3) Å, c = 12.712(2) Å, α = 112.94(1)°, β = 98.14(1)°, γ = 104.61(2)°, Z = 2; $[Sr(taci)_2(H_2O)_3]Br_2·4H_2O$, $C_{12}H_{44}Br_2N_6O_{13}Sr$, monoclinic, space group $C2/c$, a = 16.53(1) Å, b = 13.82(1) Å, c = 14.45(1) Å, β = 124.72(5)°, Z = 4; $[Ba(taci)_2(H_2O)_3]Br_2·2.25H_2O$, $C_{12}H_{40.5}BaBr_2N_6O_{11.25}$, triclinic, space group $P\bar{1}$, a = 10.187(5) Å, b = 11.189(4) Å, c = 13.210(5) Å, α = 112.84(3)°, β = 91.91(4)°, γ = 105.34(3)°, Z = 2. Cd(II) is bound to the six nitrogen donors whereas the alkaline earth metal ions are coordinated to the six hydroxyl groups of two taci molecules. An almost regular MgO_6 octahedron is observed for $[Mg(taci)_2]^{2+}$, while the CdN_6 octahedron in $[Cd(taci)_2]^{2+}$ is significantly elongated along a pseudo-3-fold axis. A coordination number of 8 for Ca(II) and of 9 for Sr(II) and Ba(II) is achieved by binding additional water molecules to these metal ions. The water molecules occupy adjacent positions in the coordination polyhedron. NMR spectroscopy and FAB^+ mass spectrometry of aqueous complex solutions revealed rather weak taci–metal interactions for the alkaline earth metal ions with decreasing stability in the order Zn, Cd ≫ Mg > Ca, Sr, Ba. The formation constants $\beta_1 = [Cd(taci)][Cd]^{-1}[taci]^{-1}$ and $\beta_2 = [Cd(taci)_2][Cd]^{-1}[taci]^{-2}$ were determined in 0.1 M KNO_3 at 25 °C and the values $\log \beta_1 = 6.48(3)$ and $\log \beta_2 = 10.95(5)$ were obtained. Molecular mechanics calculations were used to elucidate the energy of the different complexes. The calculations revealed clearly that the complex geometries and the observed coordination numbers can be understood by analyzing steric strain in the coordination sphere. On the other hand, for Mg(II), Ca(II), Sr(II), Ba(II), Zn(II), and Cd(II), the selection of one of the four possible binding sites of taci is basically a consequence of the electron configuration of the metal ion.

Introduction

A series of recent papers reported the remarkable versatility of 1,3,5-triamino-1,3,5-trideoxy-*cis*-inositol (taci) for metal binding.[2-6] Owing to four different binding sites (Chart I), taci is able to form complexes in aqueous solution with almost every metal ion. The results of these studies clearly indicated that the site as selected by a distinct metal ion is a function of, at least, two different factors: the individual affinity of the metal ion for either oxygen or nitrogen donors and the different steric requirements of the four binding modes. The preference of Al(III) for oxygen donors is well-known, and consequently, an AlO_6 coordination sphere has been observed for $[Al(taci)_2]^{3+}$. On the other hand the soft Tl(III) is exclusively bound to 6 nitrogen

Chart I[a]

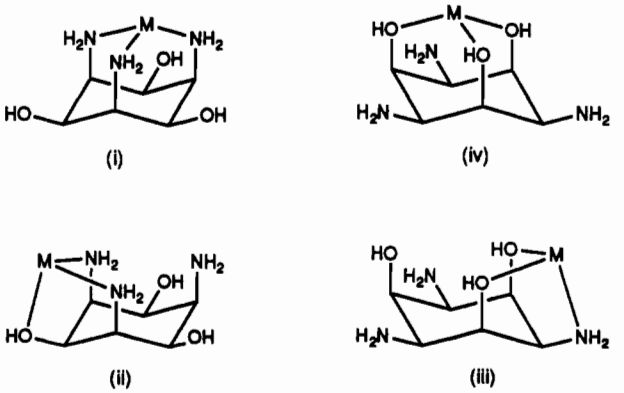

[a] The coordinated oxygen atoms in these schematic representations are shown as remaining protonated although this is not the case in their complexes with trivalent metal cations.[2,5]

* To whom correspondence should be addressed.

[⊕] Abstract published in *Advance ACS Abstracts*, October 1, 1993.

(1) (a) ETH Zürich, Laboratorium für Anorganische Chemie. (b) University of the Witwatersrand. (c) ETH, Zürich, Institut für Kristallographie und Petrographie. (d) Universität Zürich.
(2) Schmalle, H. W.; Hegetschweiler, K.; Ghisletta, M. *Acta Crystallogr.* **1991**, *C47*, 2047.
(3) Hegetschweiler, K.; Gramlich, V.; Ghisletta, M.; Samaras, H. *Inorg. Chem.* **1992**, *31*, 2341.
(4) Ghisletta, M.; Jalett, H.-P.; Gerfin, T.; Gramlich, V.; Hegetschweiler, K. *Helv. Chim. Acta* **1992**, *75*, 2233.
(5) Hegetschweiler, K.; Ghisletta, M.; Fässler, T. F.; Nesper, R.; Schmalle, H. W.; Rihs, G. *Inorg. Chem.* **1993**, *32*, 2032.
(6) Hegetschweiler, K.; Ghisletta, M.; Gramlich, V. *Inorg. Chem.* **1993**, *32*, 2699.

0020-1669/93/1332-5273$04.00/0

Table I. Potentiometric Data (25 °C, 0.1 M KNO_3) and Evaluated Formation Constants of Cd(II)–taci Complexes with Estimated Standard Deviations in Parentheses

$[Cd]_t$, mol dm^{-3}	5.05×10^{-4}	9.87×10^{-4}	9.90×10^{-4}	1.973×10^{-3}	1.977×10^{-3}	1.000×10^{-3}	2.000×10^{-3}	
$[taci]_t$, mol dm^{-3}	1.01×10^{-3}	1.974×10^{-3}	1.980×10^{-3}	3.945×10^{-3}	3.954×10^{-3}	1.020×10^{-3}	2.030×10^{-3}	
$[H]_t$, mol dm^{-3}	0	0	0	0	0	7.550×10^{-3}	1.507×10^{-2}	
titrant; [titrant], mol dm^{-3}	HNO_3; 0.1	HNO_3; 0.1	HNO_3; 0.1	HNO_3; 0.1	HNO_3; 0.1	KOH; 0.1	KOH; 0.1	
evaluated range								
equiv[a]	0.05–2.97	0.05–3.04	0.00–3.03	0.05–2.99	0.05–3.03	0.11–3.98	0.06–3.95	
pH	8.84–4.69	8.76–4.02	9.15–4.09	8.72–4.35	8.69–3.84	5.09–10.22	4.88–10.24	
no. of points	60	60	61	59	60	80	80	
$\log \beta_{xyz}$[b]								
x y z								
1 1 0	6.48	6.45	6.49	6.51	6.51	6.44	6.49	6.48(3) (av)
1 2 0	10.99	10.90	11.01	10.91	10.94			10.95(5) (av)
4 4 –4						–4.74	–4.78	–4.8(1) (av)
σ_{pH}[c]	0.0069	0.0061	0.0084	0.0039	0.0056	0.0041	0.0082	

[a] Moles of titrant/moles of taci. [b] $\beta_{xyz} = [Cd_x(taci)_yH_z][Cd]^{-x}[taci]^{-y}[H]^{-z}$. [c] $\sigma_{pH} = (\sum w(pH_{obs} - pH_{calcd})^2/\sum w)^{1/2}$; $w = (pH_{i+1} - pH_{i-1})^{-2}$.

donors, whereas the intermediate Ga(III) is simultaneously bound to 3 nitrogen and 3 oxygen donors.[5] Such a mixed N_3O_3 coordination sphere can be obtained by binding the metal ion either to the two different triaxial sites (i) and (iv) (Chart I) or to the two different axial–equatorial–axial sites (ii) and (iii). For Ga(III) a bis type (i)–type (iv) complex has been observed. Pb(II) and Bi(III) also select a mixed coordination sphere. However, these two metal ions bind to the asymmetric site (iii). It has been postulated that the particular structure of the Pb(II) and Bi(III) complexes is caused by the presence of a stereochemically active lone pair.[6]

For *cis*-inositol, the preference of a metal ion to bind either to an axial–equatorial–axial or to a triaxial site is basically a matter of the ionic radius: Large cations bind to the axial–equatorial–axial site whereas small cations bind to the triaxial site.[7] However, the differences in steric requirements and in the softness of hydroxyl and amino groups give rise to an inequality of the two different chair conformations of taci. It is thus evident that a satisfactory explanation of the site selection for taci is more complex than for *cis*-inositol. To get a closer understanding of the various metal–taci interactions, the steric requirements of the two binding modes (i) and (iv) were elucidated by molecular mechanic calculations. In the present contribution, we contrast the results of these calculations with the X-ray crystal structures of a variety of bis complexes $[M(taci)_2(H_2O)_n]^{2+}$ (M = Mg, Ca, Sr, Ba, Cd; $0 \le n \le 3$).

Experimental Section

Spectroscopy, Mass Spectrometry, and Analyses. ^1H and ^{13}C NMR spectra were measured on a Bruker AC-200 spectrometer with δ (ppm) scale and sodium (trimethylsilyl)propionate-d_4 (=0 ppm) as internal standard. The FAB^+-MS spectra were recorded on a VG ZAB VSEQ instrument. Test solutions were prepared by dissolving the samples in water and mixing the resulting solutions with a glycerol matrix prior to the introduction in the spectrometer. The isotope distribution of a peak was calculated considering all isotopes of C, H, N, Br, O, Mg, Ca, Sr, Ba, and Cd with natural abundance ≥ 0.001%. Some of the signals in the Cd complex, consisting in n individual masses, with corresponding intensities $I(j)_{obs}$, $1 \le j \le n$, were assumed to originate from the superposition of two different species $M(1)^+$ and $M(2)^+$, with corresponding isotope distributions $a(1,j)$ and $a(2,j)$. The species distribution factors x_1 and x_2 were obtained from a system of equations $I(j)_{calcd} = x_1a(1,j) + x_2a(2,j)$, by minimizing $\sum_j(I(j)_{obs} - I(j)_{calcd})^2$.[8] C, H, N, and Br analyses were performed by D. Manser, Laboratorium für Organische Chemie, ETH Zürich. Thermogravimetric analyses were measured on a Perkin-Elmer TGA 7 thermobalance, using a heating rate of 20 °C min^{-1}.

Preparation of the Complexes. taci was prepared as described in ref 4. $Cd(NO_3)_2{\cdot}4H_2O$, $MgBr_2{\cdot}6H_2O$, $Mg(ClO_4)_2{\cdot}2H_2O$, $Mg(NO_3)_2{\cdot}6H_2O$, $CaBr_2{\cdot}2H_2O$, $Sr(NO_3)_2$, $SrBr_2{\cdot}6H_2O$, $Ba(NO_3)_2$, and $BaBr_2{\cdot}2H_2O$ were commercially available products of reagent grade quality which were used without further purification. Compounds of the composition $[Cd(taci)_2](NO_3)_2{\cdot}2H_2O$ (**1**), $[Mg(taci)_2](NO_3)(OH){\cdot}6H_2O$ (**2A**), $[Mg(taci)_2]_2Br_3(OH){\cdot}9H_2O$ (**2B**), $[Mg(taci)_2]_2(ClO_4)_3(OH){\cdot}10.5H_2O$ (**2C**), $[Ca(taci)_2(H_2O)_2]Br_2{\cdot}6H_2O$ (**3**), $[Sr(taci)_2(H_2O)_3](NO_3)_2$ (**4A**), $[Sr(taci)_2(H_2O)_3]Br_2{\cdot}4H_2O$ (**4B**), $[Ba(taci)_2(H_2O)_3]Br_2{\cdot}2.25H_2O$ (**5**), and $[Ba(taci)](NO_3)_2$ (**6**) were obtained by the addition of aqueous solutions containing the corresponding metal salt (3 mmol), dissolved in a minimal amount of H_2O(3–9 mL), to an aqueous solution of taci (6 mmol in 6 mL of H_2O). **1** (77%) and **6** (65%) precipitated immediately as white solids after the combination of the two solutions. Single crystals from **1** were grown by slow cooling of the hot aqueous solution of the complex. The combination of aqueous solutions containing taci on the one hand and $Mg(NO_3)_2$ on the other resulted in the precipitation of a white solid of the composition $Mg(taci)_2(NO_3)_x(OH)_{2-x}(H_2O)_z$, where x and z were poorly reproducible. Single crystals of pure **2A** (28%) were obtained by dissolving the precipitated solid in H_2O (hot) and layering with EtOH. Single crystals of **2B** (54%) and **2C** (47%) crystallized slowly within several days from the aqueous solution (room temperature). Single crystals of **3** (56%), **4A** (33%), **4B** (59%), and **5** (64%) were grown by slow diffusion of EtOH to the aqueous complex solutions. **4A** crystallized as a hydrate $[Sr(taci)_2(H_2O)_3](NO_3)_2{\cdot}yH_2O$; however, the crystals effloresced on air yielding the above mentioned **4A** ($y = 0$). No dehydration reaction was observed in air at room temperature for the other compounds. However, in vacuo (48 h, 0.03 mbar, room temperature) **3** reacted over P_4O_{10} to form $[Ca(taci)_2(H_2O)_2]Br_2$. Extended heating of solutions containing the Sr or Ba complexes on air should be avoided, since insoluble $SrCO_3$ or $BaCO_3$ will be formed. The Mg, Ca, and Cd complex did not suffer from this problem.

Anal. Calc for $C_{12}H_{34}CdN_8O_{14}$ (**1**): C, 22.99; H, 5.47; N, 17.88. Found: C, 22.70; H, 5.67; N, 17.91. Calc for $C_{12}H_{43}MgN_7O_{16}$ (**2A**): C, 25.47; H, 7.66; N, 17.33. Found: C, 25.15; H, 7.54; N, 17.45. Calc for $C_{24}H_{79}Br_3Mg_2N_{12}O_{22}$ (**2B**): C, 24.51; H, 6.77; N, 14.29. Found: C, 25.28; H, 6.71; N, 14.02. Calc for $C_{24}H_{82}Cl_3Mg_2N_{12}O_{35.5}$ (**2C**): C, 22.84; H, 6.55; N, 13.32. Found: C, 23.38; H, 6.32; N, 13.12. Calc for $C_{12}H_{46}Br_2CaN_6O_{14}$ (**3**): C, 20.64; H, 6.64; N, 12.03. Found: C, 21.12; H, 6.40; N, 11.81. Calc for $C_{12}H_{34}Br_2CaN_6O_8$ (**3**, dried product): C, 24.42; H, 5.81; N, 14.24. Found: C, 24.24; H, 5.82; N, 14.25. Calc for $C_{12}H_{36}N_8O_{15}Sr$ (**4A**): C, 23.24; H, 5.85; N, 18.07. Found: C, 23.35; H, 5.79; N, 17.52. Calc for $C_{12}H_{44}Br_2N_6O_{13}Sr$ (**4B**): C, 19.80; H, 6.09; N, 11.54; Br, 21.95. Found: C, 20.10; H, 5.96; N, 11.39; Br, 21.91. Calc for $C_{12}H_{40.5}BaBr_2N_6O_{11.25}$ (**5**): C, 19.32; H, 5.47; N, 11.26; Br, 21.42. Found: C, 19.37; H, 5.36; N, 11.03; Br, 21.37. Calc for $C_6H_{15}BaN_3O_9$ (**6**): C, 16.43; H, 3.45; N, 15.97. Found: C, 16.49; H, 3.50; N, 15.71.

Determination of Stability Constants. In the present investigation, all equilibrium constants represent concentration quotients and pH is defined as –log[H].

The formation constants of the Cd(II)–taci complexes were determined by potentiometric measurements (25 °C, 0.1 M KNO_3).[3] Measurements with $[Cd]_t:[taci]_t = 1:2$ were performed by acidimetric titrations of solutions containing variable amounts of crystalline, analytically pure **1**. Measurements with $[Cd]_t:[taci]_t = 1:1$ were performed by alkalimetric titrations of solutions, containing $Cd(NO_3)_2$, analytically pure taci, which was free of stereoisomers according to its ^1H and ^{13}C NMR spectrum, and appropriate amounts of HNO_3. Further experimental details are summarized in Table I. Figures of the measured and calculated titration curves are available as supplementary material.

$pK_w = 13.79$ was determined by several calibration titrations.[3] The pK_w, and the pK_a's of H_3taci^{3+} (5.95, 7.40, 8.90),[3] were treated as fixed

(7) Hancock, R. D.; Hegetschweiler, K. *J. Chem. Soc., Dalton Trans.* **1993**, 2137.
(8) Korzekwa, K.; Howald, W. N.; Trager, W. F. *Biomed. Environ. Mass Spectrom.* **1990**, *19*, 211.

Table II. Crystallographic Data for taci·$2H_2O$, $[Cd(taci)_2](NO_3)_2·2H_2O$ (**1**), $[Mg(taci)_2]_2(ClO_4)_3(OH)·10.5H_2O$ (**2C**), $[Ca(taci)_2(H_2O)_2]Br_2·6H_2O$ (**3**), $[Sr(taci)_2(H_2O)_3]Br_2·4H_2O$ (**4B**), and $[Ba(taci)_2(H_2O)_3]Br_2·2.25H_2O$ (**5**)

	taci	Cd complex	Mg complex	Ca complex	Sr complex	Ba complex
chem formula	$C_6H_{19}N_3O_5$	$C_{12}H_{34}CdN_8O_{14}$	$C_{12}H_{41}Cl_{1.5}MgN_6O_{17.75}$	$C_{12}H_{46}Br_2CaN_6O_{14}$	$C_{12}H_{44}Br_2N_6O_{13}Sr$	$C_{12}H_{40.5}BaBr_2N_6O_{11.25}$
fw	213.2	626.9	631.0	698.4	728.0	746.1
cryst size, mm	0.6 × 0.5 × 0.2	0.1 × 0.4 × 0.2	0.2 × 0.2 × 0.2	0.23 × 0.55 × 0.47	0.4 × 0.16 × 0.14	0.25 × 0.12 × 0.12
space group	$P2_1/n$ (No. 14)	$P2_1/c$ (No. 14)	$P\bar{1}$ (No. 2)	$P\bar{1}$ (No. 2)	$C2/c$ (No. 15)	$P\bar{1}$ (No. 2)
cryst system	monoclinic	monoclinic	triclinic	triclinic	monoclinic	triclinic
a, Å	12.002(6)	7.110(2)	11.314(3)	10.879(2)	16.534(10)	10.187(5)
b, Å	5.506(3)	8.717(3)	11.448(3)	12.061(3)	13.822(10)	11.189(4)
c, Å	15.588(8)	18.781(7)	12.134(3)	12.712(2)	14.445(10)	13.210(5)
α, deg	90.0	90.0	111.57(2)	112.94(1)	90	112.84(3)
β, deg	97.30(3)	100.54(3)	103.16(2)	98.14(1)	124.72(5)	91.91(4)
γ, deg	90.0	90.0	105.32(2)	104.61(2)	90.0	105.34(3)
V, Å^3	1021.8(9)	1144.4(7)	1314.0(6)	1432(1)	2713(3)	1322.4(9)
diffractometer	Picker Stoe	Syntex-P21	Syntex-P21	Enraf-Nonius CAD-4	Picker-Stoe	Syntex-P21
Z	4	2	2	2	4	2
T, °C	17	20	22	22	20	25
λ, Å (Mo Kα)	0.710 73	0.710 73	0.710 73	0.710 73	0.710 73	0.710 73
ρ_{calcd}, g cm^{-3}	1.39	1.82	1.59	1.62	1.78	1.87
μ, cm^{-1}	1.11	10.40	3.11	30.43	49.98	45.50
transm coeff	0.9505/0.9627	0.6764/0.9008		0.3418/0.5851	0.3916/0.5804	0.5445/0.6580
$R(F_o)$,[a] %	4.46	4.14	7.65	6.48	4.11	3.67
$R_w(F_o)$,[b] %	4.10	5.00	9.05	6.08	4.67	4.35

[a] $R = \sum||F_o| - |F_c||/\sum|F_o|$. [b] $R_w = [\sum(|F_o| - |F_c|)^2\sum|F_o|^2]^{1/2}$; $w = 1/\sigma^2(|F_o|)$.

values and were not refined. The computer programs SUPERQUAD[9] and BEST[10] were used for the evaluation of the model and for final refinements, respectively. The evaluation of the acidimetric titrations was performed, considering the exclusive presence of the two mononuclear complexes $[Cd(taci)_2]^{2+}$ and $[Cd(taci)]^{2+}$. In the alkalimetric titration, the first buffer region $0 \le$ equiv ≤ 3 corresponded obviously to the formation of $[Cd(taci)]^{2+}$. A second buffer region $3 \le$ equiv ≤ 4 was interpreted as a deprotonation reaction of this complex. However, a significant dependence of the midpoint potential at equiv = 3.5 on $[Cd]_t$ indicated the presence of polynuclear species $[Cd_n(taci)_n(OH)_n]^{n+}$. The present data fit best for $n = 4$. However, on the basis of the available data, an unambiguous identification of the nuclearity n was not possible.

The determination of formation constants of the Mg–taci complexes was complicated by their low stability in aqueous solution. Moreover, the solubility of solids containing Mg–taci complexes was generally low. Thus, solutions of the afforded high concentration could not be prepared and therefore only a rough estimate of the formation constants could be performed. The amount of complex formation was determined by integration of the signals in the ^1H NMR spectrum in D_2O (Figure 1). The $[Mg]_t$:$[taci]_t$ ratio was varied from 1:2 to 2:1, whereby $[taci]_t$ was kept constant at 0.047 mol dm^{-3}. Assuming an exclusive formation of $[Mg(taci)]^{2+}$, the evaluated values (dm^3·mol^{-1}) for $K_1 = [Mg(taci)][Mg]^{-1}[taci]^{-1}$ (25 °C) were 0.76 ($[Mg]_t$ = 0.024 mol dm^{-3}), 0.71 ($[Mg]_t$ = 0.058 mol dm^{-3}), and 0.70 ($[Mg]_t$ = 0.094 mol dm^{-3}).

X-ray Diffraction Studies. Crystallographic data are summarized in Table II. Data collection was performed using graphite-monochromatized Mo Kα radiation. The stability of the crystals was checked by measuring standard reflections at fixed intervals during the data collection. However, no loss of intensity was noted for any of the crystals. The data were always corrected for Lorentz and polarization effects. The structures were solved using either direct methods or the Patterson interpretation routine of SHELXTL Plus (VMS)[11] and refined by full-matrix least-squares calculations. Additional experimental details on data collection, structure solution, and refinement are described in the following six paragraphs. Atomic coordinates are given in Table III. Selected, summarized bond distances and bond angles are presented in Tables IV–VI.

taci·$2H_2O$. A total of 2666 reflections were collected; 1334 were unique (R_{int} = 0.031) and 1220 were observed with $F \ge 4\sigma(F)$. A face-indexed numerical absorption correction was applied. A total of 147 parameters were refined using anisotropic displacement parameters for all non-hydrogen atoms. All hydrogen atoms were located in the difference Fourier map and were refined with variable isotropic displacement parameters.

$[Cd(taci)_2](NO_3)_2·2H_2O$ (1). A total of 1648 reflections were collected; 1509 were unique (R_{int} = 0.021), and 1304 were observed with $F \ge 4\sigma(F)$. A face-indexed numerical absorption correction was applied. A total of 160 parameters were refined using anisotropic displacement parameters for all non-hydrogen atoms. All hydrogen atomic positions could be localized in the difference Fourier map. They were included in the refinement as fixed values with fixed isotropic displacement parameters of 0.05 Å^2.

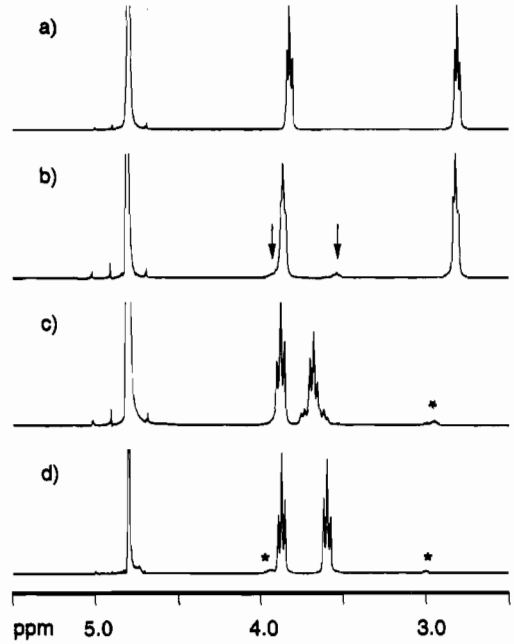

Figure 1. ^1H NMR spectra (D_2O) of (a) taci (pH 10.5), (b) $[Mg(taci)_2]^{2+}$ (pH 10.5), (c) $[Cd(taci)_2]^{2+}$ (pH 9.0), and (d) $[Zn(taci)_2]^{2+}$ (pH 8.5). The signals of the minor species are indicated with asterisks (free ligand) and with arrows (metal complexes).

$[Mg(taci)_2]_2(ClO_4)_3(OH)·10.5H_2O$ (2C). A total of 4900 reflections were collected; 4640 were unique (R_{int} = 0.010), and 2931 were observed with $F \ge 3\sigma(F)$. An absorption correction was not applied. Direct methods revealed the positions of one independent $[Mg(taci)_2]^{2+}$ molecule. The position of one Cl atom could be localized in the difference Fourier map; however, the corresponding oxygen atoms could not be assigned unambiguously. A static disorder was assumed for this ClO_4^- ion with one Cl position and eight positions for the four oxygen atoms. Fixed Cl–O distances were used to obtain realistic bond lengths. Several additional peaks, located in the difference Fourier map obviously represented a second ClO_4^- counterion and several water molecules. However, it was not possible to distinguish between Cl and O. The four oxygen positions of the second ClO_4^- ion could not be localized at all. Thus, it seems highly probable that this ClO_4^- anion and the water molecules occupy the remaining positions at random. Therefore, the most intense of the

(9) Gans, P.; Sabatini, A.; Vacca, A. *J. Chem. Soc., Dalton Trans.* **1985**, 1195.
(10) Motekaitis, R. J.; Martell, A. E. *Can. J. Chem.* **1982**, *60*, 2403.
(11) Sheldrick, G. M. *SHELXTL-PLUS 88. Structure Determination Software Programs*; Nicolet Instrument Corp.: Madison, WI, 1988.

Table III. Atomic Coordinates and Isotropic or Equivalent Isotropic Displacement Parameters with Estimated Standard Deviations in Parentheses for Non-Hydrogen Atoms of taci·2H$_2$O, [Cd(taci)$_2$](NO$_3$)$_2$·2H$_2$O (**1**), [Mg(taci)$_2$]$_2$(ClO$_4$)$_3$(OH)·10.5H$_2$O (**2C**), [Ca(taci)$_2$(H$_2$O)$_2$]Br$_2$·6H$_2$O (**3**), [Sr(taci)$_2$(H$_2$O)$_3$]Br$_2$·4H$_2$O (**4B**), and [Ba(taci)$_2$(H$_2$O)$_3$]Br$_2$·2.25H$_2$O (**5**)

atom	*x*	*y*	*z*	U_{eq}[a]/U_{iso}, Å^2	atom	*x*	*y*	*z*	U_{eq}[a]/U_{iso}, Å^2
				taci·2H$_2$O					
C(1)	−0.0818(2)	0.5368(4)	0.3123(1)	0.037(1)	N(3)	0.2284(1)	0.3769(4)	0.3690(1)	0.044(1)
C(2)	0.0263(2)	0.4552(4)	0.3675(1)	0.036(1)	N(5)	−0.0222(1)	0.2982(4)	0.0911(1)	0.051(1)
C(3)	0.1269(1)	0.4610(4)	0.3150(1)	0.036(1)	O(2)	0.0135(1)	0.2169(3)	0.4009(1)	0.047(1)
C(4)	0.1032(2)	0.3271(4)	0.2287(1)	0.037(1)	O(4)	0.0989(1)	0.0694(3)	0.2405(1)	0.043(1)
C(5)	−0.0036(2)	0.4212(4)	0.1751(1)	0.038(1)	O(6)	−0.1275(1)	0.1536(3)	0.2429(1)	0.043(1)
C(6)	−0.1047(2)	0.4015(4)	0.2268(1)	0.036(1)	O(1W)	0.3283(1)	0.7184(4)	0.4940(1)	0.072(1)
N(1)	−0.1824(1)	0.5220(4)	0.3574(1)	0.047(1)	O(2W)	0.1597(1)	0.0214(3)	0.5302(1)	0.061(1)
				[Cd(taci)$_2$](NO$_3$)$_2$·2H$_2$O (**1**)					
Cd	0.5	0.5	0.5	0.032(1)	C(3)[b]	0.2471(9)	0.7021(8)	0.5970(4)	0.031(2)
O(2)[b]	0.4565(7)	0.9138(5)	0.5861(3)	0.051(2)	C(4)[b]	0.2206(9)	0.5634(8)	0.6431(4)	0.033(2)
O(4)[b]	0.0612(6)	0.4773(5)	0.6041(3)	0.040(2)	C(5)[b]	0.3970(10)	0.4576(7)	0.6633(3)	0.031(2)
O(6)[b]	0.7287(7)	0.4486(6)	0.7087(3)	0.045(2)	C(6)[b]	0.5699(9)	0.5534(8)	0.6969(3)	0.034(3)
N(1)[b]	0.6876(7)	0.6498(6)	0.5882(3)	0.029(2)	O(1N)[b]	0.9124(10)	−0.0158(7)	0.6969(4)	0.091(3)
N(3)[b]	0.2501(7)	0.6630(6)	0.5221(3)	0.029(2)	O(2N)[b]	0.7646(8)	0.1297(7)	0.6136(3)	0.064(2)
N(5)[b]	0.4353(7)	0.3674(6)	0.6018(3)	0.031(2)	O(3N)[b]	1.0482(8)	0.1815(7)	0.6674(4)	0.082(3)
C(1)[b]	0.6109(9)	0.6922(8)	0.6533(4)	0.033(2)	N(1N)[b]	0.9073(9)	0.0994(7)	0.6590(3)	0.041(3)
C(2)[b]	0.4286(10)	0.7895(8)	0.6339(4)	0.036(3)	O(2w)[b]	0.1613(8)	0.1069(7)	0.5159(3)	0.062(2)
				[Mg(taci)$_2$]$_2$(ClO$_4$)$_3$(OH)·10.5H$_2$O (**2C**)					
Mg	0.1777(2)	0.0305(2)	0.3030(2)	0.024(1)	C(15)	0.2394(6)	−0.2400(6)	0.1122(5)	0.031(2)
O(2)	0.3281(3)	0.1055(4)	0.4704(3)	0.024(1)	C(16)	0.1178(6)	−0.2705(6)	0.1473(5)	0.031(2)
O(4)	0.0577(3)	0.0609(4)	0.4037(3)	0.025(1)	Cl(1)	0.6288(2)	0.2139(3)	0.2455(2)	0.081(1)
O(6)	0.2218(4)	0.2281(4)	0.3343(3)	0.026(1)	O(Cl1A)[c]	0.5644(7)	0.1658(10)	0.3204(7)	0.119(2)
O(12)	0.0349(4)	−0.0462(4)	0.1279(3)	0.028(2)	O(Cl2A)[c]	0.7273(8)	0.1652(11)	0.2364(8)	0.174(2)
O(14)	0.3004(4)	0.0043(4)	0.1997(3)	0.027(2)	O(Cl3A)[c]	0.5353(9)	0.1655(15)	0.1260(8)	0.319(3)
O(16)	0.1365(4)	−0.1665(4)	0.2677(4)	0.030(2)	O(Cl4A)[c]	0.6782(14)	0.3556(7)	0.3085(14)	0.413(3)
N(1)	0.4878(5)	0.3798(5)	0.5260(5)	0.035(2)	O(Cl1B)[d]	0.6686(17)	0.1126(15)	0.1792(16)	0.149(3)
N(3)	0.1906(5)	0.0721(5)	0.6391(5)	0.030(2)	O(Cl2B)[d]	0.5604(17)	0.2531(17)	0.1634(15)	0.167(3)
N(5)	0.0175(5)	0.2978(6)	0.3975(5)	0.041(2)	O(Cl3B)[d]	0.7399(12)	0.3279(12)	0.3409(13)	0.104(3)
N(11)	−0.1164(5)	−0.3168(6)	0.0832(5)	0.049(2)	O(Cl4B)[d]	0.5467(16)	0.1632(18)	0.3033(16)	0.131(3)
N(13)	0.1647(5)	−0.0166(5)	−0.0416(4)	0.035(2)	Cl(2)[e]	0.5150(4)	0.5528(4)	0.0127(4)	0.063(2)
N(15)	0.3526(5)	−0.2324(5)	0.2065(5)	0.043(2)	O(Cl21)[e]	0.4449(14)	0.5126(13)	−0.1118(8)	0.162(3)
C(1)	0.3680(6)	0.3484(6)	0.5577(5)	0.027(2)	O(Cl22)[e]	0.5880(11)	0.6927(8)	0.0819(10)	0.123(3)
C(2)	0.3430(5)	0.2217(6)	0.5801(5)	0.023(2)	O(Cl23)[e]	0.4352(13)	0.5086(11)	0.0743(11)	0.111(3)
C(3)	0.2215(5)	0.1946(6)	0.6166(5)	0.024(2)	O(Cl24)[e]	0.6082(11)	0.4877(13)	0.0153(15)	0.187(3)
C(4)	0.1010(5)	0.1833(5)	0.5201(5)	0.023(2)	O(1W)[c]	−0.1521(5)	0.5056(5)	0.1908(5)	0.035(2)
C(5)	0.1301(6)	0.3080(6)	0.4955(6)	0.027(2)	O(2W)	0.2238(6)	0.7940(6)	0.4653(5)	0.076(2)
C(6)	0.2501(6)	0.3346(6)	0.4572(5)	0.026(2)	O(3W)	0.0726(6)	0.5122(6)	0.3356(6)	0.079(2)
C(11)	−0.0028(6)	−0.2860(6)	0.0472(6)	0.033(2)	O(4W)	0.3304(5)	0.3015(5)	0.1861(5)	0.056(2)
C(12)	0.0219(6)	−0.1634(6)	0.0191(6)	0.032(2)	O(5W)	0.2796(5)	0.5302(5)	0.2473(5)	0.058(2)
C(13)	0.1455(6)	−0.1346(6)	−0.0164(6)	0.031(2)	O(6W)[e]	0.5954(12)	0.8252(15)	0.1059(11)	0.116(3)
C(14)	0.2660(6)	−0.1177(6)	0.0852(5)	0.030(2)	O(7W)[e]	0.5261(10)	0.0277(10)	0.4846(11)	0.066(2)
				[Ca(taci)$_2$(H$_2$O)$_2$]Br$_2$·6H$_2$O (**3**)					
Br(1)	0.2748(1)	0.6302(1)	0.7508(1)	0.0530(2)	N(21)	−0.3720(5)	0.6975(5)	−0.2021(5)	0.036(1)
Br(2)	0.2893(1)	0.9067(1)	0.1843(1)	0.0595(2)	N(23)	0.0144(5)	0.5735(5)	−0.1176(4)	0.026(1)
Ca	−0.1576(1)	0.7673(1)	0.1533(1)	0.0180(3)	N(25)	−0.3951(5)	0.3814(5)	−0.0372(5)	0.027(1)
O(12)	−0.2651(4)	0.9162(4)	0.1361(3)	0.0234(9)	C(21)	−0.3285(6)	0.5967(6)	−0.1903(5)	0.024(1)
O(14)	0.0111(4)	0.9635(4)	0.1856(3)	0.0204(9)	C(22)	−0.1787(5)	0.6415(6)	−0.1565(5)	0.020(1)
O(16)	−0.1415(4)	0.9253(4)	0.3509(3)	0.022(1)	C(23)	−0.1295(5)	0.5342(5)	−0.1552(5)	0.019(1)
N(11)	−0.3476(5)	1.0309(6)	0.3554(5)	0.037(1)	C(24)	−0.1877(5)	0.4760(5)	−0.0784(5)	0.019(1)
N(13)	−0.0909(5)	1.0920(5)	0.0704(4)	0.027(1)	C(25)	−0.3382(5)	0.4350(6)	−0.1127(5)	0.022(1)
N(15)	0.1234(5)	1.0903(5)	0.4397(4)	0.027(1)	C(26)	−0.3888(5)	0.5429(6)	−0.1124(5)	0.022(1)
C(11)	−0.2231(6)	1.0875(6)	0.3341(5)	0.023(1)	O(W1)	−0.2627(4)	0.6581(4)	0.2592(4)	0.037(1)
C(12)	−0.2261(6)	1.0528(6)	0.2039(5)	0.023(1)	O(W2)	0.0399(4)	0.7629(4)	0.2733(4)	0.039(1)
C(13)	−0.0939(6)	1.1193(5)	0.1929(5)	0.022(1)	O(W3)	0.5700(6)	0.7262(6)	0.3998(5)	0.068(2)
C(14)	0.0203(6)	1.0953(5)	0.2530(5)	0.020(1)	O(W4)	0.4956(5)	0.8815(5)	−0.0012(6)	0.073(2)
C(15)	0.0221(6)	1.1243(6)	0.3822(5)	0.022(1)	O(W5)	0.0200(6)	0.6153(5)	0.4010(5)	0.068(2)
C(16)	−0.1125(6)	1.0604(6)	0.3962(5)	0.024(1)	O(W6)	0.3591(6)	0.8246(6)	0.4147(5)	0.082(2)
O(22)	−0.1267(4)	0.7538(4)	−0.0439(3)	0.0220(9)	O(W7)[f]	0.6517(9)	0.6538(10)	0.5712(9)	0.159(4)
O(24)	−0.1340(4)	0.5640(4)	0.0448(3)	0.0212(9)	O(W8A)[f,g]	0.2698(9)	0.5891(9)	0.4724(8)	0.077(3)
O(26)	−0.3627(4)	0.6407(4)	0.0051(3)	0.0224(9)	O(W8B)[f,h]	0.2184(17)	0.5198(18)	0.4933(15)	0.072(5)
				[Sr(taci)$_2$(H$_2$O)$_3$]Br$_2$·4H$_2$O (**4B**)					
Sr	0.5	0.1157(1)	0.25	0.022(1)	C(2)[i]	0.4382(6)	0.1306(6)	−0.0373(7)	0.023(4)
Br[i]	0.1588(1)	−0.0895(1)	−0.0685(1)	0.049(1)	C(3)[i]	0.3577(6)	0.2069(6)	−0.0754(7)	0.026(5)
O(2)[i]	0.4523(4)	0.0741(4)	0.0531(4)	0.025(3)	C(4)[i]	0.3883(6)	0.2886(6)	0.0101(7)	0.024(5)
O(4)[i]	0.3962(4)	0.2552(4)	0.1091(5)	0.026(3)	C(5)[i]	0.4865(6)	0.3343(6)	0.0433(7)	0.026(5)
O(6)[i]	0.6005(4)	0.2191(4)	0.1894(4)	0.027(3)	C(6)[i]	0.5687(6)	0.2595(6)	0.0824(7)	0.026(5)
N(1)[i]	0.6107(5)	0.1024(5)	0.0351(6)	0.028(4)	O(1W)[i]	0.3167(4)	0.0503(4)	0.1537(5)	0.041(4)
N(3)[i]	0.2642(5)	0.1625(5)	−0.1044(6)	0.033(4)	O(2W)	0.5	−0.0726(6)	0.25	0.039(5)
N(5)[i]	0.5230(5)	0.4115(5)	0.1291(6)	0.036(4)	O(3W)[i]	0.1890(5)	−0.0295(5)	−0.2756(5)	0.055(4)
C(1)[i]	0.5356(6)	0.1777(6)	−0.0032(7)	0.025(5)	O(4W)[i]	0.1618(5)	−0.3016(5)	−0.1710(6)	0.061(5)
				[Ba(taci)$_2$(H$_2$O)$_3$]Br$_2$·2.25H$_2$O (**5**)					
Ba	0.7010(1)	0.0980(1)	0.2310(1)	0.027(1)	O(23)	0.5293(5)	−0.3129(4)	0.0578(3)	0.025(2)
Br(1)	0.4645(1)	0.2903(1)	0.4042(1)	0.047(1)	O(25)	0.6438(5)	−0.0362(4)	0.0529(4)	0.027(2)
Br(2)	−0.1166(1)	0.2463(1)	0.8510(1)	0.060(1)	N(22)	0.6830(6)	−0.4832(6)	−0.0599(5)	0.036(2)
O(11)	0.7229(5)	0.1750(5)	0.3496(4)	0.031(2)	N(24)	0.3721(6)	−0.2076(6)	−0.0521(5)	0.032(2)
O(13)	0.9509(5)	0.0858(5)	0.2434(4)	0.028(2)	N(26)	0.8625(6)	−0.0429(6)	−0.0883(5)	0.030(2)
O(15)	0.8597(5)	0.0206(5)	0.4351(4)	0.028(2)	C(21)	0.7783(7)	−0.2600(7)	−0.0725(6)	0.028(2)
N(12)	0.9094(7)	0.3438(7)	0.2714(5)	0.045(2)	C(22)	0.6535(7)	−0.3860(7)	−0.0998(6)	0.029(2)
N(14)	1.1422(6)	0.0787(6)	0.4083(5)	0.034(2)	C(23)	0.5230(7)	−0.3542(7)	−0.0607(5)	0.025(2)
N(16)	0.7579(7)	0.2352(7)	0.5813(5)	0.043(2)	C(24)	0.4930(7)	−0.2471(7)	−0.0948(6)	0.028(2)
C(11)	0.8357(8)	0.2881(7)	0.4253(6)	0.032(2)	C(25)	0.6154(7)	−0.1195(7)	−0.0649(5)	0.028(2)
C(12)	0.9564(8)	0.3178(7)	0.3651(6)	0.031(2)	C(26)	0.7413(7)	−0.1598(7)	−0.1105(6)	0.027(2)
C(13)	1.0313(8)	0.2105(7)	0.3327(6)	0.029(2)	O(2)	0.5546(7)	−0.2390(8)	0.3518(6)	0.091(2)
C(14)	1.0717(7)	0.1845(7)	0.4344(6)	0.029(2)	O(3)	0.4384(6)	−0.0500(6)	0.2643(5)	0.062(2)
C(15)	0.9544(7)	0.1555(7)	0.4965(6)	0.029(2)	O(4)	0.8043(6)	−0.3094(6)	0.2278(5)	0.054(2)
C(16)	0.8784(8)	0.2635(7)	0.5246(6)	0.031(2)	O(5)	0.7357(6)	−0.4880(6)	0.3286(5)	0.058(2)
O(21)	0.8329(5)	−0.1940(5)	0.0453(4)	0.027(2)	O(6)	0.7287(7)	−0.4956(6)	−0.3517(5)	0.072(2)
					O(7)[d]	0.9595(24)	0.4385(21)	0.0985(18)	0.072(3)

[a] $U_{eq} = {}^1/_3\sum_i\sum_j U_{ij}a_i^*a_j^*a_i a_j$. [b] Symmetry-related atoms are generated by the operation $1-x, 1-y, 1-z$. [c] Occupancy factor = 0.75. [d] Occupancy factor = 0.25. [e] Occupancy factor = 0.5. [f] Refined isotropically. [g] Occupancy factor = $^2/_3$. [h] Occupancy factor = $^1/_3$. [i] Symmetry-related atoms are generated by the symmetry operation $1-x, y, 0.5-z$.

Table IV. Summarized Bond Distances (Å) of taci·$2H_2O$, $[Cd(taci)_2](NO_3)_2·2H_2O$ (**1**), $[Mg(taci)_2]_2(ClO_4)_3(OH)·10.5H_2O$ (**2C**), $[Ca(taci)_2(H_2O)_2]Br_2·6H_2O$ (**3**), $[Sr(taci)_2(H_2O)_3]Br_2·4H_2O$ (**4B**), and $[Ba(taci)_2(H_2O)_3]Br_2·2.25H_2O$ (**5**)

	M–OH_2	M–O(taci)	M–N	C–C	C–N	C–O
			taci			
min				1.522(3)	1.465(2)	1.421(3)
max				1.543(3)	1.474(3)	1.433(3)
av				1.533	1.468	1.427
			Cd Complex			
min			2.329(5)	1.52(1)	1.452(9)	1.438(8)
max			2.370(5)	1.548(9)	1.473(9)	1.443(7)
av			2.350	1.532	1.463	1.441
			Mg Complex			
min		2.032(4)		1.515(9)	1.45(1)	1.430(6)
max		2.080(5)		1.54(1)	1.493(9)	1.440(6)
av		2.047		1.528	1.472	1.435
			Ca Complex			
min	2.432(4)	2.389(4)		1.514(8)	1.462(8)	1.429(7)
max	2.477(5)	2.524(4)		1.544(8)	1.475(7)	1.451(6)
av	2.455	2.439		1.526	1.467	1.437
			Sr Complex			
min	2.603(8)	2.548(7)		1.53(1)	1.47(1)	1.42(1)
max	2.672(7)	2.688(8)		1.54(1)	1.49(1)	1.44(1)
av	2.649	2.616		1.53	1.48	1.43
			Ba Complex			
min	2.819(7)	2.704(4)		1.51(1)	1.464(8)	1.436(6)
max	2.880(7)	2.814(5)		1.55(1)	1.49(1)	1.452(8)
av	2.850	2.764		1.53	1.473	1.445

Table V. Selected, Summarized Bond Angles (deg) of $[Cd(taci)_2](NO_3)_2·2H_2O$ (**1**) and $[Mg(taci)_2]_2(ClO_4)_3(OH)·10.5H_2O$ (**2C**)[a]

angle	min	max	av
N–Cd–N	82.5(2)	83.6(2)	83.2
N–Cd–N′ (*cis*)	96.4(2)	97.5(2)	96.8
N–Cd–N′ (*trans*)	180.0	180.0	180.0
Cd–N–C	117.1(4)	118.7(4)	117.9
O–Mg–O	84.0(2)	88.2(2)	86.3
O–Mg–O′ (*cis*)	91.9(2)	95.7(2)	93.7
O–Mg–O′ (*trans*)	176.1(2)	178.4(2)	177.6
C–O–Mg	120.7(3)	123.0(3)	121.8

[a] Intraligand angles are indicated as X–M–X; interligand angles are indicated as X–M–X′ (X = N, O; M = Mg, Cd).

Table VI. Selected, Summarized Bond Angles (deg) of $[Ca(taci)_2(H_2O)_2]Br_2·6H_2O$ (**3**), $[Sr(taci)_2(H_2O)_3]Br_2·4H_2O$ (**4B**), and $[Ba(taci)_2(H_2O)_3]·Br_2·2.25H_2O$ (**5**)

	O–M–O[a]	O′–M–O[b]	M–O–C	O–M–O(W)[c]	O(W)–M–O(W)[d]	O(W)–M–O(W)[e]
			Ca Complex			
min	70.6(1)	70.6(1)	126.5(3)	70.9(1)	80.3(2)	
max	74.8(1)	144.1(1)	130.1(3)	147.0(1)	80.3(2)	
av	72.5	114.0	129.1	105.2	80.3	
			Sr Complex			
min	66.9(2)	66.9(2)	130.1(5)	67.7(2)	70.2(1)	140.4(3)
max	69.5(2)	153.9(2)	133.3(4)	137.7(2)	70.2(1)	140.4(3)
av	67.9	112.5	131.5	102.9	70.2	140.4
			Ba Complex			
min	62.8(2)	67.1(1)	130.3(4)	66.8(1)	68.2(2)	133.0(2)
max	67.5(1)	153.0(2)	131.9(5)	143.9(2)	68.3(2)	133.0(2)
av	65.6	114.4	131.2	103.4	68.3	133.0

[a] Two hydroxyl groups of the same taci molecule. [b] Two hydroxyl groups of two different taci molecules. [c] One hydroxyl group of a taci molecule and one coordinated water molecule. [d] Two adjacent, coordinated water molecules. [e] Two remote, coordinated water molecules.

remaining peaks in the difference Fourier map was assigned to the Cl position of the second ClO_4^- ion with an occupancy factor of 0.5. Four oxygen positions were calculated with fixed Cl–O distances and fixed O–Cl–O angles. The other peaks were interpreted as water molecules and the required OH^- ion for charge balance. A total of 416 parameters were refined using anisotropic displacement parameters for the non-hydrogen atoms. All 30 hydrogen atoms of the $[Mg(taci)_2]^{2+}$ molecule appeared in the difference Fourier map. However, some of the bond distances and bond angles did not fall in the expected range. Therefore, calculated positions (riding model) with fixed isotropic displacement parameters of 0.05 Å^2 were used in the refinement.

$[Ca(taci)_2(H_2O)_2]Br_2·6H_2O$ (3). A total of 8770 reflections were collected; 6599 were unique (R_{int} = 0.016), and 4413 were observed with $F \geq 6\sigma(F)$. A face-indexed numerical absorption correction was applied (nine crystal faces). A total of 310 parameters were refined using anisotropic displacement parameters for all non-hydrogen atoms of the $[Ca(taci)_2(H_2O)_2]Br_2$ entity. Four of the remaining six water molecules were also refined using anisotropic displacement parameters for the oxygen positions, whereas O(W7) and O(W8) were refined isotropically. The displacement parameter of O(W8) was unusually high. Since two peaks were observed for O(W8) in the difference electron density map, showing an intensity ratio of 2:1, the position was split in O(W8A) (occupancy factor = $^2/_3$) and O(W8B) (occupancy factor = $^1/_3$). All hydrogen atoms of the $[Ca(taci)_2(OH_2)_2]^{2+}$ entity and 11 of the 12 hydrogen atoms of the additional 6 water molecules were located in the difference Fourier map. These positions were included in the refinement as fixed values with constant isotropic displacement parameters of 0.03 Å^2 for H(–C), H(–N), and H(–O) of the ligand molecules and 0.05 Å^2 for the H(–O) positions of the water molecules.

$[Sr(taci)_2(H_2O)_3]Br_2·4H_2O$ (4B). A total of 1870 reflections were collected; 1780 were unique (R_{int} = 0.00), and 1486 were observed with $F \geq 4\sigma(F)$. A face-indexed numerical absorption correction was applied. A total of 155 parameters were refined using anisotropic displacement parameters for all non-hydrogen atoms. The H(–O), H(–N), and H(–C) hydrogen positions of taci could be localized in the difference Fourier map and were refined as fixed values with fixed isotropic displacement parameters of 0.05 Å^2.

$[Ba(taci)_2(H_2O)_3]Br_2·2.25H_2O$ (5). A total of 3706 reflections were collected; 3469 were unique (R_{int} = 0.038), and 3112 were observed with $F \geq 4\sigma(F)$. A face-indexed numerical absorption correction was applied. In addition to the $[Ba(taci)_2(H_2O)_3]^{2+}$ complex and the two Br^- counterions, two water molecules were found. An additional weak peak in the difference Fourier map was interpreted as a third water molecule. However, its oxygen atom appeared to have an abnormal high displacement parameter and was therefore refined with an occupancy factor of 0.25. Elemental analysis confirmed the presence of two rather than three additional water molecules in the crystal. A total of 298 parameters were used in the final refinement with anisotropic displacement parameters for all non-hydrogen atoms. All H(–O), H(–N), and H(–C) hydrogen positions of the two taci molecules could be localized in the difference Fourier map. They were refined as fixed values with fixed isotropic displacement parameters of 0.05 Å^2 for H(–N) and H(–O) and 0.08 Å^2 for H(–C).

Molecular Mechanics Calculations. These were carried out using the commercially available program SYBYL.[12] The scans of strain energy as a function of metal ion radius were carried out as described previously.[13] The program SYBYL generates the geometry around the metal ion by use of van der Waals repulsion between the donor atoms, rather than by specifying bond angles and force constants for the metal ion and its donor atoms. The scans were therefore carried out using this mode. All torsional force constants about the metal–ligand bonds were set to zero. An ideal angle of 109.5° and an angle bending force constant of 0.059 kJ·mol^{-1}·deg^{-1} was used for the M–N–C and M–O–C angles, and a constant M–N or M–O bond stretching constant of 837 kJ·mol^{-1}·Å^{-1} was used. The results of the calculations are not particularly sensitive to the value of the M–L force constant used.[13] All other parameters in the calculations were as contained in the TRIPOS 5.2 force field in SYBYL.[12] A validation of this force field is found in ref 14. No charges were calculated on the atoms of the metal–taci complexes. The scans are presented as a function of metal radius. The radius[15] of metal ions appears from the available data to be related quite well to M–N and M–O bond lengths by the relation M–N bond length = ionic radius +1.43 Å and by M–O bond length = ionic radius + 1.37 Å. The scans of strain energy versus metal ion radius seen in Figures 5–7 were thus drawn up on this basis. In order to minimize the problem of false energy minima, the molecular dynamics module of SYBYL was used. Each structure of a taci complex that had been generated by the DRAW model building module of SYBYL was energy minimized and then subjected to a 10 000 fs run on the molecular dynamics module DYNAMICS. The file containing the energy of the

(12) SYBYL Program, available from TRIPOS Associates, 1699 South Hanley Road, St. Louis, MO 63144.
(13) Hancock, R. D. *Prog. Inorg. Chem.* **1989**, *37*, 187.
(14) Clark, M.; Cramer, R. D.; Van Opdenbosch, N. *J. Comput. Chem.* **1989**, *10*, 982.
(15) Shannon, R. D. *Acta Crystallogr.* **1976**, *A32*, 751.

complex as a function of time was examined, with low energy structures extracted from this file, and the energy was minimized once more. In many cases this procedure revealed no structures of lower energy than the initial structure, although in a few cases structures of considerably lower energy were located. This procedure was particularly important in calculating the structures of the hydrated forms of bis type (iv) complexes where up to three water molecules coordinated to the metal ion were present, as there was considerable plasticity in the coordination sphere.

Results

Preparation and Characterization of the Solid Compounds. Crystalline compounds containing the bis complexes of the four alkaline-earth-metal ions and of Cd(II) were readily obtained in aqueous medium by the addition of a solution of an appropriate metal salt to a solution of the ligand. Elemental analyses of the solid compounds revealed the incorporation of 2–8 equiv of water/equiv of complex. The dehydration and degradation of the solid Ca, Sr, and Ba complexes **3**, **4B**, and **5** were performed by thermogravimetry. The three compounds exhibited a similar decomposition behavior. All thermal decompositions occurred in two steps. For the Sr and Ba compound, the first decrease in weight corresponds to the loss of 7.0 equiv or 5.3 equiv of water, respectively. According to elemental analysis and X-ray data, these values indicate a complete dehydration of the compounds. The dehydration of the Ca complex started already below 50 °C. All three dehydration reactions were completed at about 200 °C. It is interesting to note that under the experimental conditions used in the present investigation, no evidence for the formation of stable compounds with an intermediate degree of hydration was found. The Ca and Sr complexes showed a second decrease in weight of 176 and 179 mass units, respectively, at 300–350 °C. These values are in agreement with the loss of one ligand (177 mass units): $M(taci)_2Br_2 \cdot xH_2O \rightarrow M(taci)_2Br_2 \rightarrow M(taci)Br_2$. The second step of the Ba compound occurred in two substeps at 250 and 300 °C. Moreover, the loss of about 160 mass units indicates the elimination of 2 equiv of HBr rather than of one ligand: $Ba(taci)_2Br_2 \cdot 5.25H_2O \rightarrow Ba(taci)_2Br_2 \rightarrow Ba(H_{-1}taci)_2$. The thermogravimetric degradation curves are available as supplementary material. In contrast to the thermogravimetric measurements, drying at room temperature resulted in the formation of well-defined compounds with an intermediate degree of hydration. The formation of $Ca(taci)_2Br_2 \cdot 2H_2O$ and $Sr(taci)_2(NO_3)_2 \cdot 3H_2O$ (**4A**) was verified by elemental analysis.

NMR Spectroscopy and Potentiometric Measurements. The ^1H NMR spectra of the free ligand and the Cd(II), Zn(II), and Mg(II) complexes are presented in Figure 1. The spectra of the Ca(II), Sr(II), and Ba(II) complexes were identical with that of the free ligand. The main component in the spectrum of the Mg(II) complex corresponds also to that of the free ligand, however, an additional minor species (5% abundance) exhibiting two separate signals with characteristic downfield shifts was also observed. It is reasonable to regard this species as a Mg(II)–taci complex. The presence of only two signals clearly indicate the binding of Mg^{2+} to the site (iv) of taci. The available data did not allow an unambiguous determination of the corresponding stoichiometry. A 1:1 or a 1:2 complex or even a mixture of both, as indicated by the FAB MS,[16] must be taken into account. However, the obviously low stability of this species makes a 1:1 complex more likely. In fact, the NMR data fit better for a 1:1 than for a 1:2 complex. The corresponding formation constant $[Mg(taci)][Mg]^{-1}[taci]^{-1}$ of 0.7 ± 0.2 mol^{-1} dm^3 can be estimated by using the equilibrium concentrations obtained by integration of the NMR signals. In contrast to the alkaline earth metal complexes, the spectrum of a 0.01 M $[Cd(taci)_2]^{2+}$ solution in D_2O exhibited only a marginal amount of free ligand. Moreover, the chemical shifts of the Cd and the Mg complex were different.

(16) It should be noted that the volatile H_2O evaporated mostly prior to the bombardment and ionization of the sample. Thus, the observed peaks in the mass spectrum correspond to the species distribution in glycerol rather than in H_2O.

Table VII. FAB^+ MS Data for $[Cd(taci)_2](NO_3)_2 \cdot 2H_2O$ (**1**), $[Zn(taci)_2]Br_2 \cdot 4H_2O$,[a] $[Mg(taci)_2](NO_3)(OH) \cdot 6H_2O$ (**2A**), $[Ca(taci)_2(H_2O)_2]Br_2 \cdot 6H_2O$ (**3**), $[Sr(taci)_2(H_2O)_3]Br_2 \cdot 4H_2O$ (**4B**), and $[Ba(taci)_2(H_2O)_3]Br_2 \cdot 2.25H_2O$ (**5**) (Glycerol (=glyc) Matrix)

	intensities (%)					
assgnt	Cd	Zn[a]	Mg	Ca	Sr	Ba
$[H(taci)]^+$	67	22	100	100	100	100
$[M(taci) - H]^+$	23	38	6	6	15	13
$[M(taci)]^+$	71	28				
$[M(taci)(glyc) - H]^+$	43		5	9	12	5
$[M(taci)X]^+$	22	100	4			
$[M(taci)_2 - H]^+$	100	80	22	2		4
$[M(taci)_2X]^+$	23	17	2			
$[M(glyc) - H]^+$			6	20	24	30
$[M(glyc)_2 - H]^+$			5	48	28	19
$[M(glyc)_2X]^+$			7	16	16	12
$[M(glyc)_3 - H]^+$				18	11	7
$[M(glyc)_3X]^+$				10	12	8
$[M(glyc)_4 - H]^+$				5	3	3
stability quotient[b]	1.00	1.00	0.68	0.13	0.22	0.22

[a] From ref 3. [b] Σ(intensity of metal taci complexes)/Σ(intensity of metal-containing ions).

The spectrum of the $[Cd(taci)_2]^{2+}$ is, however, closely related to that of the previously reported Zn complex,[3] where a bis type (i) structure has been assigned in solution. The rather small difference in chemical shifts between the two signals prevented an unambiguous assignment of H–(C–N) and H–(C–O) in the previous study. However, the observation of Cd satellites clearly allows now an unambiguous assignment of H–(C–N) to the signal observed at higher field. It seems quite likely that the same assignment is also correct for the Zn complex.

The stability constans of $[Cd(taci)]^{2+}$ and $[Cd(taci)_2]^{2+}$ in aqueous solution were determined by potentiometric measurements (25 °C, 0.1 M KNO_3). The values $\log \beta_1 = 6.48(3)$ and $\log \beta_2 = 10.95(5)$ were obtained. These are in good agreement with the 3% amount of free taci detected by NMR in the 0.01 M complex solution.

Mass Spectrometry. FAB^+ mass spectra of the metal complexes were obtained by the use of aqueous complex solutions and glycerol as matrix. In the spectrum of the Cd complex, peaks of metal-containing ions were readily recognized by the characteristic isotope distribution of Cd. The two most intense signals at $m/z = 289.0$ and $m/z = 467.1$ were assigned to a 1:1 and a 1:2 complex. The observed isotope pattern of the latter peak was in good agreement with the calculated isotope pattern of $[Cd(taci)_2 - H]^+$ (see also Figure S2, supplementary data), whereas the fit of the first peak for a 1:1 complex was remarkably poor. However, a satisfactory agreement between the calculated and observed pattern could be obtained by assuming a superposition of the two ions $[Cd(taci) - H]^+$ and $[Cd(taci)]^+$. Least-squares calculations indicated that a 1:3 ratio of these two ions was present. Thus, monopositive ions were obviously generated from $[Cd(taci)]^{2+}$ by two independent processes: (1) dissociation of a proton from the ligand and (2) uptake of an electron by Cd(II). A comparison of the spectra of the Cd and Zn complexes clearly shows that the formation of monovalent Cd is favored: The ratio of intensities $[M^I(taci)]^+ : [M^{II}(taci) - H]^+$ is 3 for Cd but only 0.74 for Zn.[3] Additional peak assignments are given in Table VII.

In contrast to Cd, the taci complexes of the alkaline earth metals were of rather low abundance (Table VII). A comparison of observed intensities clearly indicates that these metals appeared mainly bound to a variable number of glycerol molecules.[16]

X-ray Diffraction Studies: Characterization of Tautomers. The crystal structure of $taci \cdot 2H_2O$, $[Cd(taci)_2](NO_3)_2 \cdot 2H_2O$ (**1**), $[Ca(taci)_2(H_2O)_2]Br_2 \cdot 6H_2O$ (**3**), $[Sr(taci)_2(H_2O)_3]Br_2 \cdot 4H_2O$ (**4B**), and $[Ba(taci)_2(H_2O)_3]Br_2 \cdot 2.25H_2O$ (**5**) could be solved and refined without difficulties. Single crystals of the three different compounds **2A–C**, containing the Mg(II) complex with either NO_3^-, Br^-, or ClO_4^- as counterion, were subjected to X-ray analysis. Although the non-hydrogen atoms of the $[Mg(taci)_2]^{2+}$

Scheme I

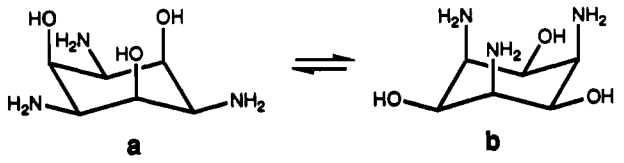

molecule refined well for all three compounds, a high degree of disorder was found for the counterions and several water molecules. Only the crystal of the perchlorate proved to be of sufficient quality for a satisfactory structure analysis. However, the $[Mg(taci)_2]^{2+}$ molecules, as found in the three different compounds, exhibited essentially the same structure.[17] The bond lengths and bond angles of the ligand fall in the expected range, and the Mg–O lengths compared well with those of other Mg complexes reported in the literature.[18-20] According to elemental analysis, the compounds contain either OH^- or a deprotonated taci molecule bearing an alkoxo group. The present X-ray data do not allow one to establish the position of this negative charge. Since all protons of the coordinated hydroxyl groups of $H_{-1}[Mg(taci)_2]_2(ClO_4)_3 \cdot 11.5H_2O$ were located, **2C** was formulated as $[Mg(taci)_2]_2(ClO_4)_3(OH) \cdot 10.5H_2O$. However, a structure with a coordinated alkoxo group, i.e. $[Mg(taci)_2][Mg(H_{-1}taci)(taci)](ClO_4)_3 \cdot 11.5H_2O$, where the missing proton is statistically distributed over all four ligand molecules, must also be taken into account.

In the present investigation, particular attention was given to the question whether the binding of a divalent metal ion M(II) to the hydroxyl groups resulted in a proton transfer according to $(H_2N-)_3C_6H_6(-OH)_3 + M \rightarrow (H_3N-)_3C_6H_6(-O-)_3M$. The crystals of the Ca, Sr, and Ba complexes were of sufficient quality and size to unambiguously locate all H–N and H–O protons in the $M(taci)_2^{2+}$ fragments. The results clearly indicate that Ca(II), Sr(II), and Ba(II) are coordinated to the six hydroxyl groups of two taci molecules and the above mentioned proton transfer does not occur. Also for the Mg complex, all hydrogen atoms of the complex molecule were localized in the difference electron density map, showing again the presence of six coordinated OH groups and of six NH_2 groups. However, some of the bond distances and angles were in poor agreement with the expected values. Thus, this result is not as unambiguous as those for the other alkaline earth metal complexes.

Molecular Structure of the Free Ligand. MM calculations showed that the two chair conformations **a** and **b** are the most stable (Scheme I). According to these calculations, both conformers are stabilized by hydrogen bonds between the three axial substituents. Thus, the repulsion due to having OH or NH_2 groups in axial position is quite small compared to having, for example, a methyl group. Conformer **a** with three axial hydroxyl groups is slightly favored by about 2 kJ·mol^{-1}. However, it is important to note that these calculations were carried out for an isolated molecule and solvation effects have not been taken into account. Nevertheless, the MM results were in agreement with the observed X-ray structure, showing the expected chair conformation with three axial hydroxyl groups, as well as strong intramolecular hydrogen bonding between two of the three hydroxyl groups (Figure 2).

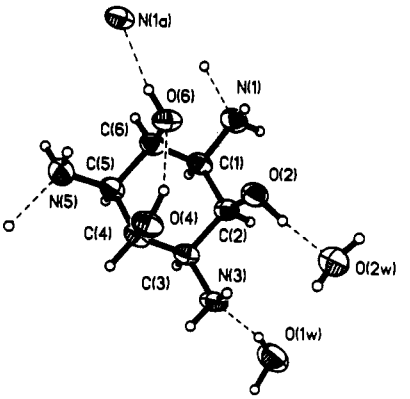

Figure 2. ORTEP plot of taci·$2H_2O$ with numbering scheme and vibrational ellipsoids at the 50% probability level.

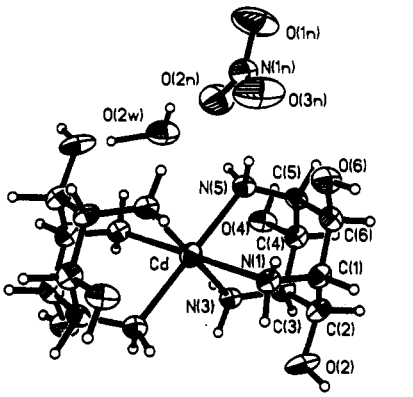

Figure 3. ORTEP plot of $[Cd(taci)_2](NO_3)_2 \cdot 2H_2O$ (**1**) with numbering scheme and vibrational ellipsoids at the 50% probability level.

Molecular Structure of the Metal Complexes. The X-ray structure of the Cd complex is shown in Figure 3. The Cd atom is located on a center of symmetry and binds to six nitrogen donors of two taci molecules, forming an approximately octahedral CdN_6 coordination sphere with a significant trigonal distortion. This distortion is indicated by intraligand angles N_i–Cd–$N_j < 90°$ and interligand angles N_i–Cd–$N_j' > 90°$. It can be regarded as a stretching of the octahedron along the pseudo-3-fold axis. The Cd–N bond lengths fall in the usual range expected for a Cd amine complex with a coordination number of 6.[21-23]

Mg(II), Ca(II), Sr(II), and Ba(II) bind all to the six hydroxyl groups of two taci molecules (Figure 4), i.e. site (iv) in Chart I. The NH_2 groups of taci are neither protonated nor coordinated. Ideally, the molecular symmetry would be D_{3d} for the Mg complex and C_2 for the Ca and Sr complexes. However, only the Sr complex has an imposed crystallographic symmetry (C_2): Sr

(17) (a) $[Mg(taci)_2](NO_3)(OH) \cdot 6H_2O$ (**2A**), space group $P2_1$, $a = 11.908(5)$ Å, $b = 16.878(8)$ Å, $c = 13.369(9)$ Å, $\beta = 114.63(4)°$, $Z = 4$, 998 observed reflections with $I \geq 2\sigma(I)$, 178 refined parameters, $R = 0.147$, Mg–O = 2.03(3)–2.09(3) Å (average: 2.065 Å). (b) $[Mg(taci)_2]_2Br_3(OH) \cdot 9H_2O$ (**2B**): space group $P2_1/n$, $a = 6.933(2)$ Å, $b = 14.045(3)$ Å, $c = 12.856(3)$ Å, $\beta = 98.24(3)°$, $Z = 2$, 1461 observed reflections with $I \geq 2\sigma(I)$, 169 refined parameters, $R = 0.157$, Mg–O = 2.02(1)–2.06(1) Å (average:2.046 Å).

(18) Poonia, N. S.; Bajaj, A. V. *Chem. Rev.* **1979**, *79*, 389.

(19) An average Mg–O bond lengths of 2.065 Å was calculated from a total of 27 structures providing an octahedral MgO_6 entity. $[Mg(H_2O)_6]^{2+}$: (a) Schier, A.; Gamper, S.; Müller, G. *Inorg. Chim. Acta* **1990**, *177*, 179. (b) Gupta, M. P.; Van Alsenoy, C.; Lenstra, A. T. H. *Acta Crystallogr.* **1984**, *C40*, 1526. (c) $[Mg(OC(NH_2)_2)_6]^{2+}$: Lebioda, L.; Stadnicka, K.; Sliwinski, J. *Acta Crystallogr.* **1979**, *B35*, 157. (d) $[Mg(CH_3COOC_2H_5)_6]^{2+}$: Utko, J.; Sobota, P.; Lis, T.; Majewska, K. *J. Organomet. Chem.* **1989**, *359*, 295. (e) $[Mg(DMF)_6]^{2+}$: Pulla Rao, C.; Muralikrishna Rao, A.; Rao, C. N. R. *Inorg. Chem.* **1984**, *23*, 2080. (f) $[Mg(C_2H_5OH)_6]^{2+}$: Valle, G.; Baruzzi, G.; Paganetto, G.; Depaoli, G.; Zannetti, R.; Marigo, A. *Inorg. Chim. Acta* **1989**, *156*, 157. (g) $[Mg(THF)_6]^{2+}$: Sobota, P.; Pluziński, T.; Lis, T. Z. *Anorg. Allg. Chem.* **1986**, *533*, 215. For complexes with multidentate ligands, see e.g.: (h) Groth, P. *Acta Chem. Scand.* **1987**, *A41*, 178. (i) Joesten, M. D.; Hussain, M. S.; Lenhert, P. G. *Inorg. Chem.* **1970**, *9*, 151.

(20) (a) Lewinski, K.; Lebioda, L. *J. Am. Chem. Soc.* **1986**, *108*, 3693. (b) Cole, L. B.; Holt, E. M. *J. Chem. Soc., Perkin Trans. 2* **1986**, 1997.

(21) (a) Breitwieser, M.; Göttlicher, S.; Paulus, H. *Z. Kristallogr.* **1984**, *166*, 207. (b) Shi-Xiong, L.; Jin-Ling, H. *Acta Chim. Sin.* **1986**, *44*, 288.

(22) (a) Strasdeit, H.; Saak, W.; Pohl, S.; Driessen, W. L.; Reedijk, J. *Inorg. Chem.* **1988**, *27*, 1557 and references therein. (b) Ito, H.; Ito, T. *Acta Crystallogr.* **1985**, *C41*, 1598. (c) Drew, M. G. B.; McFall, S. G.; Nelson, S. M. *J. Chem. Soc., Dalton Trans.* **1979**, 575. (d) Paap, F.; Erdonmez, A.; Driessen, W. L.; Reedijk, J. *Acta Crystallogr.* **1986**, *C42*, 783.

(23) (a) Bencini, A.; Bianchi, A.; Castelló, M.; Di Vaira, M.; Faus, J.; Garcia-España, E.; Micheloni, M.; Paoletti, P. *Inorg. Chem.* **1989**, *28*, 347. (b) Adam, K. R.; McCool, B. J.; Leong, A. J.; Lindoy, L. F.; Ansell, C. W. G.; Baillie, P. J.; Dancey, K. P.; Drummond, L. A.; Henrick, K.; McPartlin, M.; Uppal, D. K.; Tasker, P. A. *J. Chem. Soc., Dalton Trans.* **1990**, 3435.

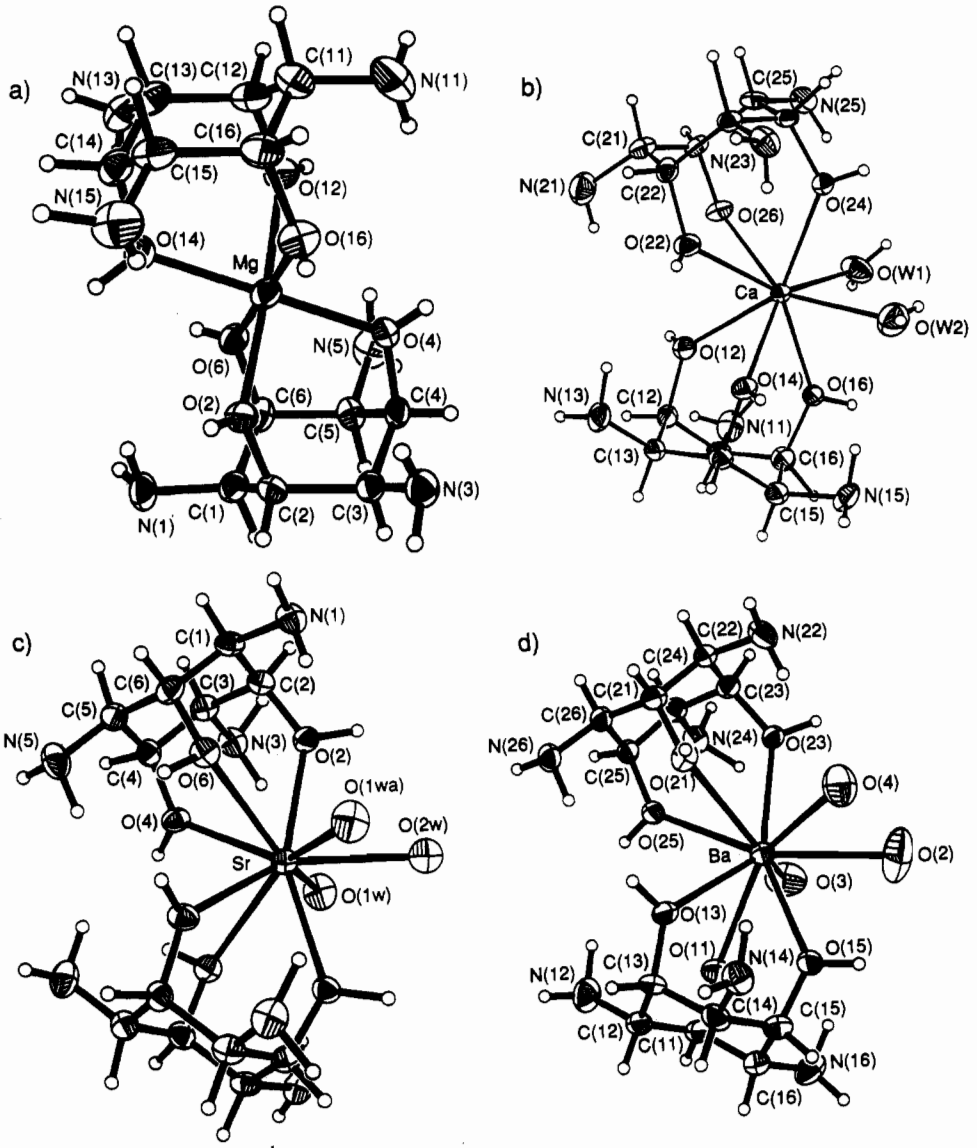

Figure 4. ORTEP plots of (a) $[Mg(taci)_2]^{2+}$, (b) $[Ca(taci)_2(H_2O)_2]^{2+}$, (c) $[Sr(taci)_2(H_2O)_3]^{2+}$, and (d) $[Ba(taci)_2(H_2O)_3]^{2+}$ with numbering schemes and vibrational ellipsoids at the 50% probability level.

and O(2w) are located on a 2-fold axis. The six oxygen donors of the Mg complex lie at the vertices of an almost regular octahedron. The coordination spheres of the Ca, Sr, and Ba complexes are completed by two (Ca) or three (Sr, Ba) additional water molecules, which are placed on adjacent positions in the coordination polyhedron. The geometry of the Ca complex can be described as a square antiprism: {O(24), O(W2), O(14), O(22)} and {O(26), O(W1), O(16), O(12)} define two almost parallel, slightly distorted squares. The geometry of the Sr complex can be regarded as a slightly distorted, tricapped, trigonal prism: O(2w), O(6a), and O(6) cap the three rectangular faces of the prism, formed by the two triangles {O(2), O(4), O(1w)} and {O(1wa), O(2a), O(4a)}. The irregular coordination polyhedron of the Ba complex may be described as a very distorted monocapped square antiprism. O(21) is capping the rectangle formed by O(4), O(13), O(25), and O(23).

The Ca–O,[18,20,24-27] Sr–O,[18,26,28,29] and Ba–O[18,27,30-32] bond lengths compare well with the corresponding values, reported in literature. However, it is interesting to note that the M–OH_2 bond lengths are generally longer than the corresponding M–OH_{taci} distances.

Systematic differences in the structures of the four alkaline earth metal complexes can be summarized as follows:

(a) The coordination numbers (Mg, 6; Ca, 8; Sr, 9; Ba, 9) increase with increasing ionic size. In fact, these numbers represent the most common one,[18-20,24-32] although other values

(24) An average Ca–O bond length of 2.44 Å was calculated from a total of 12 structures with an eight-coordinated Ca^{2+}. See e.g. (a) Schauer, C. K.; Anderson, O. P. *J. Chem. Soc., Dalton Trans.* **1989**, 185. (b) Smith, G.; O'Reilly, E. J.; Kennard, C. H. L.; White, A. H. *J. Chem. Soc., Dalton Trans.* **1985**, 243. (c) Singh, T. P.; Reinhardt, R.; Poonia, N. S. *Inorg. Nucl. Chem. Lett.* **1980**, *16*, 293. (d) Rogers, R. D.; Bond, A. H.; Hipple, W. G. *J. Cryst. Spectrosc. Res.* **1990**, *20*, 611.

(25) (a) Schauer, C. K.; Anderson, O. P. *J. Am. Chem. Soc.* **1987**, *109*, 3646. (b) Skoulika, S.; Michaelides, A.; Aubry, A. *Acta Crystallogr.* **1988**, *C44*, 931.

(26) Wei, Y. Y.; Tinant, B.; Declercq, J.-P.; Van Meerssche, M. *Acta Crystallogr.* **1987**, *C43*, 1274.

(27) Sheldrick, B.; Mackie, W.; Akrigg, D. *Acta Crystallogr.* **1989**, *C45*, 191.

(28) An average Sr–O bond length of 2.66 Å was calculated from a total of 7 structures with a nine-coordinated Sr^{2+}: (a) Baggio, R. F.; De Perazzo, P. K.; Polla, G. *Acta Crystallogr.* **1985**, *C41*, 194. (b) Burns, J. H.; Kessler, R. M. *Inorg. Chem.* **1987**, *26*, 1370.

(29) Angyal, S. J.; Craig, D. C.; Defaye, J.; Gadelle, A. *Can. J. Chem.* **1990**, *68*, 1140.

(30) An average Ba–O bond length of 2.82 Å was obtained from a total of 7 structures with a nine-coordinated Ba^{2+}: (a) Sivý, P.; Koreň, B.; Valach, F.; Lukeš, I. *Acta Crystallogr.* **1989**, *C45*, 23. (b) Starynowicz, P. *Acta Crystallogr.* **1991**, *C47*, 32. (c) Sauer, N. N.; Garcia, E.; Salazar, K. V.; Ryan, R. R.; Martin, J. A. *J. Am. Chem. Soc.* **1990**, *112*, 1524. (d) Van Der Sluis, P.; Spek, A. L.; Timmer, K.; Meinema, H. A. *Acta Crystallogr.* **1990**, *C46*, 1741. (e) Suh, I.-H.; Aoki, K.; Yamazaki, H. *Acta Crystallogr.* **1989**, *C45*, 415. (f) Burns, J. H. *Inorg. Chim. Acta* **1985**, *102*, 15.

(31) Burns, J. H.; Bryan, S. A. *Acta Crystallogr.* **1988**, *C44*, 1742.

(32) Van Staveren, C. J.; van Eerden, J.; van Veggel, F. C. J. M.; Harkema, S.; Reinhoudt, D. N. *J. Am. Chem. Soc.* **1988**, *110*, 4994.

Table VIII. Characteristic Structural Properties in the Bis Complexes $[M(taci)_2(H_2O)_x]^{2+}$ of the Alkaline Earth Metal Ions ($0 \le x \le 3$): Puckering Parameters[a] Q (Å), θ (deg), ϕ (deg); Angle ξ[b] (deg) between Mean Planes; Average Intraligand O–M–O Angle α (deg); Average C–O–M Angle β (deg)

	Q	θ	ϕ	ξ	α	β
Mg				178.1	86.3	121.8
ring 1	0.57	2.7	−12.9			
ring 2	0.55	1.1	−59.2			
Ca				138.1	72.5	129.1
ring 1	0.53	−3.2	215.6			
ring 2	0.55	1.5	−36.0			
Sr[c]	0.53	0.8	154.9	130.6	67.9	131.5
Ba				132.8	65.6	131.2
ring 1	0.52	−1.4	221.7			
ring 2	0.53	4.4	−81.2			

[a] According to Cremer and Pople.[50] [b] For definition, see Chart II. [c] Ring 1 and ring 2 are symmetry-equivalent due to a crystallographic C_2 axis.

are also known: Ba^{2+}, 8–12;[18,33] Sr^{2+}, 6, 8–10;[18,34] Ca^{2+}, 6–10;[18,35] Mg^{2+}, 4–8.[18,36,37]

(b) The increasing ionic radius gives rise to a decrease of the angles O–M–O and an increase of the angle C–O–M within the M–taci fragment (Table VIII). Obviously, the binding of the large Ca^{2+}, Sr^{2+}, and Ba^{2+} cations to the site (iv) of taci induces severe steric strain. Some of this strain is probably absorbed by the above mentioned shortening of the $M–OH_{taci}$ distances and also by a flattening of the cyclohexane ring, as indicated by a steady decrease of the puckering amplitude Q with increasing ionic radius. The amount of steric strain has been calculated by MM calculations. These calculations reveal that the optimal metal ion size for a bis type (iv) complex is slightly smaller than that of Mg^{2+}. The strain energy in a hypothetical $[Ba(taci)_2]^{2+}$ complex has been estimated to be >100 kJ/mol (Figure 5).

(c) The presence of additional coordinated water molecules in a $M(taci)_2$ complex causes a loss of coplanarity between the mean planes of the two cyclohexane rings (see Chart II). The angles between these planes in the complexes reported here are presented in Table VIII. A steady increase of this effect is observed with an increasing number of coordinated water molecules.

Discussion

Structural Properties. A comparison of the structure of the Zn(II)[3] and Cd(II) complexes on the one hand and of the Mg(II), Ca(II), Sr(II), and Ba(II) complexes on the other hand is particularly interesting, since Mg^{2+} (r = 0.72 Å) and Zn^{2+} (r = 0.74 Å) as well as Ca^{2+} (r = 1.00 Å) and Cd (r = 0.95 Å) have comparable ionic radii.[15] Similar structures of related Ca and Cd complexes,[25] as well as of related Mg and Zn complexes,[36] have frequently been reported. A comparison of the average bond lengths in the bis taci complexes shows indeed similar values

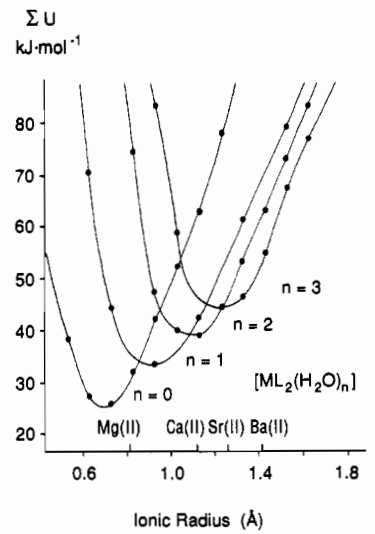

Figure 5. MM calculations for the bis–type (iv) taci complexes formed by alkaline earth metal ions, where taci (=L) is bound to the metal in the trihydroxo–triamino form. Strain energy is plotted as a function of the ionic radius for complexes with varying numbers (n) of water molecules, bound to the metal as indicated. The ionic radii of the metal ions Mg(II) through Ba(II) predict correctly the numbers of coordinated water molecules found on the bis type (IV) complexes in this work.

Chart II

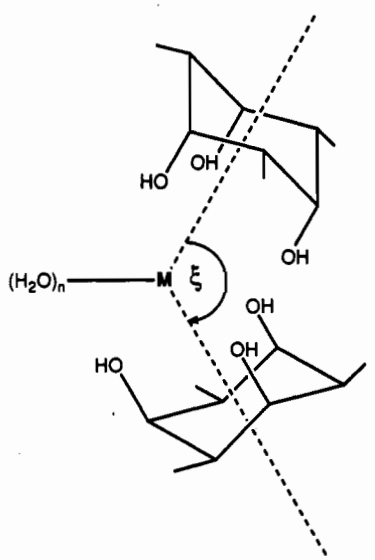

for Zn–N (2.19 Å)[3] and Mg–O (2.05 Å) as well as for Cd–N (2.35 Å) and Ca–O (2.44 Å). The exclusive binding of the group IIB elements to nitrogen donors and of the group IIA elements to oxygen donors is a clear consequence of the d^{10}-electron configuration, making a group IIB cation a softer Lewis acid. Consequently, the binding of the hydroxyl groups to the alkaline earth metal cations must be regarded mainly as an electrostatic interaction, whereas the binding of the nitrogen donors to Zn(II) and Cd(II) is much more covalent. This model is clearly supported by comparing systematic differences in the observed structures: As a consequence of the severe steric strain, the binding of the large cations to the triaxial sites of taci results in a decrease of the intraligand N–M–N and O–M–O angles (Chart III). However, this effect is much more pronounced for Ca than for Cd. Moreover, in the Ca, Sr, and Ba complexes, part of the strain is absorbed by a widening of the C–O–M angle (up to 131° for Ba). However, the C–N–M angle is not directly correlated with ionic size (Table IX). For the known complexes with a bis type (i) structure, a rather small range (116–119°) of this angle has been observed. These values are only slightly larger than those expected for an sp^3 nitrogen atom.

(33) For a ten-coordinated Ba^{2+}, see: (a) Venkatasubramanian, K.; Poonia, N. S.; Clinger, K.; Ernst, S. R.; Hackert, M. L. *J. Inclusion Phenom.* **1984**, *1*, 319. (b) Van Staveren, C. J.; Reinhoudt, D. N.; van Eerden, J.; Harkema, S. *J. Chem. Soc., Chem. Commun.* **1987**, 974. (c) van Veggel, F. C. J. M.; Harkema, S.; Bos, M.; Verboom, W.; Woolthuis, G. K.; Reinhoudt, D. N. *J. Org. Chem.* **1989**, *54*, 2351. See also ref 32. For an eleven-coordinated Ba^{2+}, see: (d) Chandler, C. J.; Gable, R. W.; Gulbis, J. M.; Mackay, M. F. *Aust. J. Chem.* **1988**, *41*, 799. (e) van Veggel, F. C. J. M.; Bos, M.; Harkema, S.; van de Bovenkamp, H.; Verboom, W.; Reedijk, J.; Reinhoudt, D. N. *J. Org. Chem.* **1991**, *56*, 225.

(34) For a eight-coordinated Sr^{2+} see: (a) Jones, P. G. *Acta Crystallogr.* **1984**, *C40*, 804. (b) Fenton, D. E.; Parkin, D.; Newton, R. F.; Nowell, I. W.; Walker, P. E. *J. Chem. Soc., Dalton Trans.* **1982**, 327. See also ref 29. For a ten-coordinated Sr^{2+}, see ref 31.

(35) (a) For a nine-coordinated Ca^{2+}, see: Neupert-Laves, K.; Dobler, M. *J. Cryst. Spectr. Res.* **1982**, *12*, 287. (b) For a ten-coordinated Ca^{2+}, see: Dyer, R. B.; Metcalf, D. H.; Ghirardelli, R. G.; Palmer, R. A.; Holt, E. M. *J. Am. Chem. Soc.* **1986**, *108*, 3621.

(36) For a seven-coordinated Mg^{2+}, see: Kennard, C. H. L.; Smith, G.; O'Reilly, E. J.; Reynolds, B. J.; Mak, T. C. W. *J. Chem. Soc., Dalton Trans.* **1988**, 2357.

(37) For a eight-coordinated Mg^{2+}, see e.g.: Owen, J. D. *Acta Crystallogr.* **1983**, *C39*, 579.

Chart III

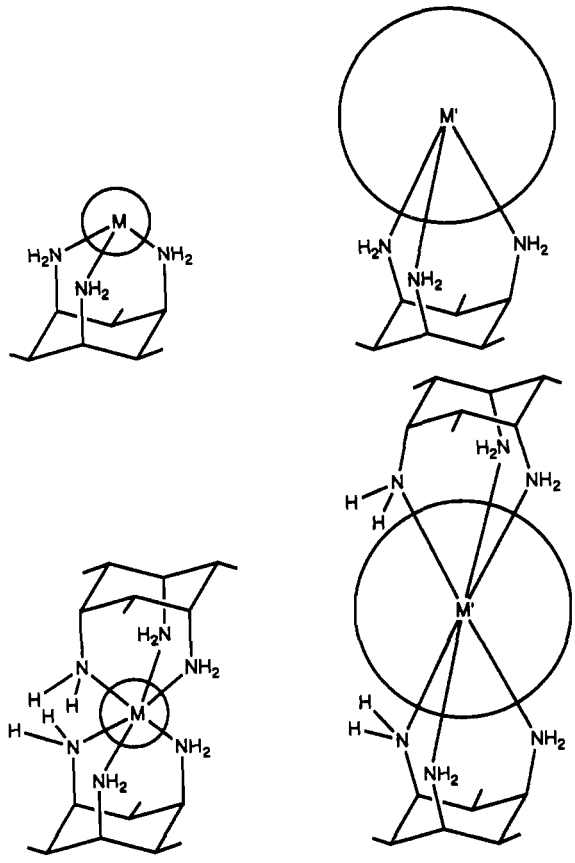

Table IX. Characteristic Structural Properties of Bis Type (i) $[M(taci)_2]^{z+}$ Complexes (z = 2, 3)

metal ion	M–N, Å	N–M–N,[a] deg	C–N–M, deg
Cd^{2+}	2.35	83.2	117.9
Tl^{3+}	2.32	84.9	116.3[b]
Zn^{2+}	2.19	87.3	116.8[c]
Co^{3+}	2.00	89.7	119.4[d]

[a] Intraligand angle. [b] Data from ref 5. [c] Data from ref 3. [d] Data from ref 4.

The different coordination numbers of Ca and Cd can be explained by the different steric requirements of the hydroxyl groups and the amino groups. Although Cd(II) generally shows a lower tendency to reach high coordination numbers,[38,39] a value of 7 or 8 is not unusual,[40] particularly when nitrato ligands are present. However, in $[Cd(taci)_2](NO_3)_2 \cdot 2H_2O$ (**1**), the nitrates do not coordinate to Cd and act only as counterions. Also the two incorporated water molecules are not bound to the metal. MM calculations clearly revealed a much lower affinity for a bis type (i) complex to bind additional water molecules compared with a corresponding bis type (iv) complex (Figures 5 and 7). Since MM calculations consider only steric requirements (electronic properties of metal–ligand bonding are not taken into account), the excellent prediction of the observed coordination numbers by the MM calculations indicates that the coordination numbers of the IIA and IIB metal taci complexes are basically determined by steric strain in the ligand sphere.

Stability of the Alkaline Earth Metal Complexes. Johnstone and Rose investigated complex formation of alkali cations with macrocyclic ligands by FAB^+ mass spectrometry using aqueous sample solutions and glycerol as matrix.[41] The authors reported that the observed peaks in the spectrum closely reflect the species distribution in solution. In the present investigation, FAB^+ mass spectrometry of the taci complexes was performed under similar experimental conditions.[16] However, our results demonstrate that such correlations are not generally applicable when reduction of the metal cation must be taken into account, as demonstrated for the reaction Cd(II) → Cd(I). Nevertheless, in the case of the alkaline earth metal complexes, FAB MS proved to be a valuable tool for the elucidation of complex formation in solution. Since the dominant peaks refer to simple glycerol complexes, the interaction of taci with alkaline earth metal cations must be considered as generally weak. The stability of these complexes decreases in the order Zn > Cd ≫ Mg > Ca, Sr, Ba (Table VII), as also indicated by the NMR data. Thus, the isolation of bis complexes in the solid compounds does not indicate a predominance of these species in solution at all. This result rather reflects a particularly favored packing in the crystal. When $Ba(NO_3)_2$ instead of $BaBr_2$ was used, the 1:1 complex **6** was isolated from aqueous solution.

It is interesting to compare taci with the structurally related *cis*-inositol. The formation constant $\beta_1 = [Mg(taci)][Mg]^{-1}[taci]^{-1} = 0.72 \pm 0.2$ dm^3·mol^{-1}, as estimated from the NMR data, is in excellent agreement with the corresponding value of 0.6 dm^3·mol^{-1} observed by Angyal for *cis*-inositol.[42] However, in contrast to taci, *cis*-inositol shows an increased affinity for the larger Ca^{2+} and Sr^{2+}.[43] This increased affinity has been explained by different site selection: Mg^{2+} binds to the triaxial site of *cis*-inositol whereas Ca and Sr bind to one of the three eq–ax–eq sites.[42] In accordance with this observation, MM calculations revealed a drastic increase of steric strain for the binding of large cations to the triaxial site.[7] However, in the case of taci, this effect is obviously overcompensated by the strong preference of the hard d^0 ions for oxygen donors (Chart I).

The taci complexes of the large alkaline earth cations are stabilized by the coordination of additional water molecules (Figure 5). However, according to the thermogravimetric measurements, which showed a complete dehydration of the Ca, Sr, and Ba compounds below 150–200 °C, these coordinated water molecules are easily detached from the metal ions. It is interesting to note that a discrimination between the water of crystallization and water of coordination was not possible by this method. However, drying of **3** and **4A** at room temperature resulted in the formation of the well-defined solids $Ca(taci)_2Br_2 \cdot 2H_2O$ and $Sr(taci)_2(NO_3)_2 \cdot 3H_2O$, where the intermediate degree of hydration corresponded exactly to the number of water molecules bound to the metal.

Stability of $[Cd(tacl)_2]^{2+}$ vs $[Zn(tacl)_2]^{2+}$. The comparison of the formation constants of $[Cd(taci)_2]^{2+}$, $[Cd(taci)]^{2+}$, $[Zn(taci)_2]^{2+}$, and $[Zn(taci)]^{2+}$ with those of other Cd(II) and Zn-

(38) Fujita, T.; Ohtaki, H. *Bull. Chem. Soc. Jpn.* **1980**, *53*, 930.
(39) (a) Ansell, C. W. G.; McPartlin, M.; Tasker, P. A.; Thambythurai, A. *Polyhedron* **1983**, *2*, 83. (b) Cannas, M.; Carta, G.; Cristini, A.; Marongiu, G. *J. Chem. Soc., Dalton Trans.* **1976**, 210.
(40) For a seven-coordinated Cd(II) see: (a) Mosset, A.; Galy, J.; Munoz-Roca, C.; Beltran-Porter, D. *Z. Kristallogr.* **1987**, *181*, 83. (b) Kleywegt, G. J.; Wiesmeijer, W. G. R.; Van Driel, G. J.; Driessen, W. L.; Reedijk, J.; Noordik, J. H. *J. Chem. Soc., Dalton Trans.* **1985**, 2177. (c) Solans, X.; Font-Altaba, M.; Oliva, J.; Herrera, J. *Acta Crystallogr.* **1985**, *C41*, 1020. (d) Drew, M. G. B.; Hollis, S.; McFall, S. G.; Nelson, S. M. *J. Inorg. Nucl. Chem.* **1978**, *40*, 1595. (e) Flook, R. J.; Freeman, H. C.; Moore, C. J.; Scudder, M. L. *J. Chem. Soc., Chem. Commun.* **1973**, 753. (f) Solans, X.; Font-Bardia, M.; Aguiló, M.; Arostegui, M.; Oliva, J. *Acta Crystallogr.* **1987**, *C43*, 648. (g) Griffith, E. A. H.; Charles, N. G.; Lewinski, K.; Amma, E. L.; Rodesiler, P. F. *Inorg. Chem.* **1987**, *26*, 3983. (h) Nelson, S. M.; McFall, S. G. *J. Chem. Soc., Chem. Commun.* **1977**, 167. For an eight-coordinated Cd, see: (i) Voissat, B.; Khodadad, P.; Rodier, N. *Acta Crystallogr.* **1984**, *C40*, 24. (j) Adam, K. R.; Donnelly, S.; Leong, A. J.; Lindoy, L. F.; McCool, B. J.; Bashall, A.; Dent, M. R.; Murphy, B. P.; McPartlin, M.; Fenton, D. E.; Tasker, P. A. *J. Chem. Soc., Dalton Trans.* **1990**, 1635. (k) Strasdeit, H.; Pohl, S. *Z. Naturforsch.* **1988**, *43b*, 1579. (l) Nakasuka, N.; Azuma, S.; Tanaka, M. *Acta Crystallogr.* **1986**, *C42*, 1736. (m) Epstein, J. M.; Dewan, J. C.; Kepert, D. L.; White, A. H. *J. Chem. Soc., Dalton Trans.* **1974**, 1949. See also ref 25.
(41) Johnstone, R. A. W.; Rose, M. E. *J. Chem. Soc., Chem. Commun.* **1983**, 1268.
(42) Angyal, S. J.; Hickman, R. *J. Aust. J. Chem.* **1975**, *28*, 1279.
(43) $\beta_1 = [ML][M]^{-1}[L]^{-1}$ (dm^3·mol^{-1}), $\beta_2 = [ML_2][M]^{-1}[L]^{-2}$ (dm^6·mol^{-2}); L = *cis*-inositol. M = Ca^{2+}: $\beta_1 = 9 \pm 3$, $\beta_2 = 450 \pm 150$. M = Sr^{2+}: $\beta_1 = 6 \pm 2$, $\beta_2 = 250 \pm 50$. Values are from ref 42.

Table X. Comparison of the Stability of Cd(II) and Zn(II) Complexes with Aliphatic and Alicyclic Amines

ligand		Zn	Cd	$\Delta G_{Cd} - \Delta G_{Zn}$, kJ mol^{-1}
	Three Nitrogen Donors			
taci[a]	log β_1	8.4	6.5	11.0
NH_3[b]	log β_3	7.1	6.2	5.4
[9]aneN_3[c]	log β_1	11.6	9.4	12.6
[10]aneN_3[d]	log β_1	11.3	8.8	14.3
2,2-tri[e]	log β_1	8.8	8.3	2.9
2,3-tri[f]	log β_1	8.6	7.8	4.7
3,3-tri[g]	log β_1	7.9	6.6	7.5
	Six Nitrogen Donors			
taci[a]	log β_2	13.6	11.0	14.9
en[h]	log β_3	12.6	11.6	5.7
2,3-tri[f]	log β_2	12.4	11.5	5.1
penten[i]	log β_1	16.2	16.1	0.8
[18]aneN_6[j]	log β_1	17.8	17.9	−0.6

[a] 1,3,5-Triamino-1,3,5-trideoxy-*cis*-inositol, 25 °C, I = 0.1. Cd complexes: this work. Zn complexes: ref 3. [b] 25 °C, I = 1.[44] [c] 1,4,7-Triazacyclononane, 25 °C, I = 0.1.[44] [d] 1,4,7-Triazacyclodecane, 25 °C, I = 0.1.[44] [e] 1,4,7-Triazaheptane, 25 °C, I = 0.1.[44] [f] 1,4,8-Triazaoctane, 25 °C, I = 0.1.[44] [g] 1,5,9-Triazanonane, 25 °C, I = 0.1.[44] [h] 1,2-Diaminoethane, 25 °C, I = 0.1, ref.[44] [i] 4,7-Bis(2′-aminoethyl)-1,4,7,10-tetraazadecane, 20 °C, I = 0.1.[47] [j] 1,4,7,10,13,16-Hexaazacyclooctadecane, 25 °C, I = 0.1.[44]

(II) amine complexes is presented in Table X. It is well-known that Cd(II) generally forms slightly less stable complexes with aliphatic polyamines than Zn(II).[45] The corresponding ΔG value of the Zn(II) complex is usually 4–8 kJ mol^{-1} more negative than for the corresponding Cd(II) complex. Close examination of the available data indicate that this is basically an entropy effect. ΔS_{Zn} is generally more positive than ΔS_{Cd}, whereas differences in ΔH are rather small and often the Cd complex is slightly favored.[45] Two exceptions of this general trend are indicated in Table X: The triazacycloalkanes [9]aneN_3 and [10]aneN_3 show a particular preference Zn(II) over Cd(II) due to a less favorable ΔH_{Cd}.[46] This has been explained by increased steric strain in the complex with the large Cd(II). On the other hand, the Zn(II) and Cd(II) complexes of the hexadentate "penten" have about the same stability.[47] Moreover, an inversion of the sequence $K_{ZnL} > K_{CdL}$ has been found for a variety of macrocyclic ligands.[48] Such anomalies have been explained by different structures of the Zn(II) and Cd(II) complexes in solution.[23,47,48] It is well-known that Cd has a greater tendency to exhibit higher coordination numbers than Zn.[49] However, the NMR data, presented in this investigation (Figure 1), in combination with the X-ray data, strongly support related structures for $[Zn(taci)_2]^{2+}$ and $[Cd(taci)_2]^{2+}$ in aqueous solution. Thus, the enhanced discrimination $\beta_{Zn(taci)_2} > \beta_{Cd(taci)_2}$ of taci must be understood on the basis of an unfavorable ΔH_{Cd}, caused by increased steric strain analogously to the above mentioned triazacycloalkanes. The different steric strain for $[Zn(taci)_2]^{2+}$ and $[Cd(taci)_2]^{2+}$ has been elucidated by molecular mechanic calculations. The strain energy of a hypothetical M(taci) complex as a function of the ionic radius of the metal ion M is presented in Figure 6. Binding to the site (i) of taci results in the exclusive formation of six-membered chelate rings in a chair conformation and favors the binding of very small metal ions like Be^{2+}, V^{5+}, or Ge^{4+}. For such a complex, the optimal N–M–N angle is 109.5°.

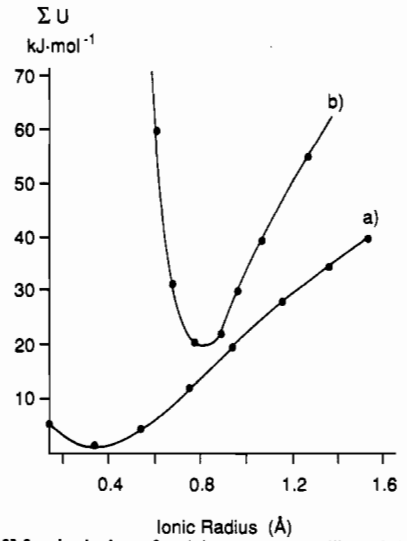

Figure 6. MM calculations for (a) mono-type (i) and (b) bis type (i) taci complexes. Strain energy is plotted as a function of the ionic radius.

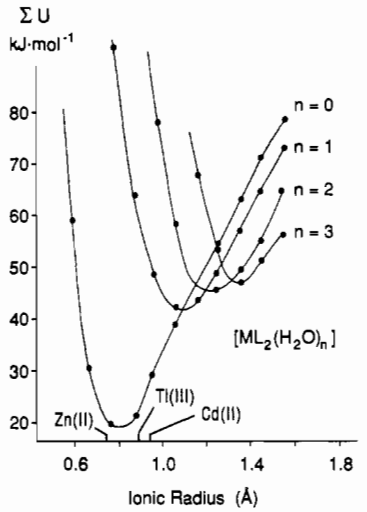

Figure 7. MM calculations for bis-type (i) complexes. Strain energy is plotted as a function of the ionic radius for complexes with a varying number of additional water molecules, bound to the metal ion as indicated. The much greater difficulty in coordinating extra water molecules to bis-type (i) complexes, as compared with the bis-type (iv) complexes shown in Figure 5, is due to the greater steric crowding produced by NH_2 groups as compared to OH groups coordinated to the metal ion.

Table IX presents some values of N–M–N angles in $[M(taci)_2]^{z+}$ complexes, together with the corresponding M–N bond lengths. As can be seen there, an increase of the M–N bond length (i.e. ionic radius) causes a steady decrease of the N–M–N bond angle. In the bis type (i) complexes additional interligand van der Waals repulsions between the N–H hydrogen atoms must be considered (Chart III). The repulsion between these N–H hydrogen atoms causes a rapid rise in strain energy below an M–N length of about 2.2 Å. Therefore, the optimal ionic radius shifts from 0.35 Å for a mono type (i) complex to 0.8 Å for a bis type (i) complex (Figures 6 and 7). Thus, Zn(II), with a ionic radius of 0.74 Å, is about the best-fit size for the bis type (i) complex of taci. However, Cd(II), with a Cd–N length of 2.35 Å, is too large to fit in a bis type (i) complex without strain. The difference $\Delta H_{Cd} - \Delta H_{Zn}$, due to increased steric strain for Cd, has been calculated to be 8.5 kJ/mol. This value is in good agreement with the observed difference $\Delta G_{Cd} - \Delta G_{Zn}$ of 14.9 kJ/mol (Table X).

Conclusions

The present investigation, together with results of previous contributions, suggests the classification of metal ions M^{z+} into five categories with respect to the observed structures in their taci complexes:

(44) Martell, A. E.; Smith, R. M. *Critical Stability Constants*; Plenum Press: New York, 1974–1989; Vols. 1–6.
(45) Anderegg, G.; Bläuenstein, P. *Helv. Chim. Acta* **1982**, *65*, 913.
(46) Kodama, M.; Kimura, E. *J. Chem. Soc., Dalton Trans.* **1978**, 1081.
(47) Schwarzenbach, G.; Moser, P. *Helv. Chim. Acta* **1953**, *36*, 581.
(48) Adam, K. R.; Dancey, K. P.; Leong, A. J.; Lindoy, L. F.; McCool, B. J.; McPartlin, M.; Tasker, P. A. *J. Am. Chem. Soc.* **1988**, *110*, 8471.
(49) Zn(II) forms a tetrahedral $Zn(NH_3)_4^{2+}$ and Cd(II) an octahedral $Cd(NH_3)_6^{2+}$ in concentrated aqueous NH_3 solutions. For Zn, see: Yamaguchi, T.; Ohtaki, H. *Bull. Chem. Soc. Jpn.* **1978**, *51*, 3227. For Cd, see: Yamaguchi, T.; Ohtaki, H. *Bull. Chem. Soc. Jpn.* **1979**, *52*, 1223.
(50) Cremer, D.; Pople, J. A. *J. Am. Chem. Soc.* **1975**, *97*, 1354.

(1) Metal ions with a d^0 electron configuration and $z \leq +2$ form mononuclear bis complexes. The ions bind to the three hydroxyl groups (site iv) of taci. The hydroxyl groups remain protonated. Additional water molecules may complete the coordination sphere depending on the size of the metal ion. The complexes must be regarded as rather weak associates which largely decay in dilute aqueous solutions. Examples: Mg^{2+}, Ca^{2+}, Sr^{2+}, Ba^{2+}.

(2) d^0 metal ions with $z \geq 3$, as well as hard trivalent transition metal ions with a d^q electron configuration, $1 \leq q \leq 5$, also form mononuclear bis complexes and bind to the oxygen donors of taci. However, due to the higher charge, a proton transfer from OH to NH_2 takes place; i.e., the metal ion is exclusively bonded to six alkoxo groups. The coordination number is always 6. These complexes are usually very stable. Examples: Al^{3+}, Cr^{3+}, Ti^{4+}.

(3) Divalent transition metal ions with a d^q electron configuration, $1 \leq q \leq 9$, divalent d^{10} metal ions, and sufficiently large trivalent d^{10} metal ions form mononuclear bis complexes having an MN_6 coordination sphere. The metal ions are exclusively coordinated to the amino groups of taci. The complexes are quite stable in aqueous solution, as expected for an alicyclic triamine. The coordination number is generally 6. Examples: Ni^{2+}, Cu^{2+}, Zn^{2+}, Cd^{2+}, Tl^{3+}.

(4) Some of the trivalent transition metal ions with a d^q electron configuration, $1 \leq q \leq 9$, and small trivalent d^{10} metal ions form mononuclear bis complexes having an MN_3O_3 coordination sphere obtained by the combination of the modes (i) and (iv). Clearly, this category represents an intermediate case between categories (2) and (3). The coordination number is exclusively 6. The three coordinated hydroxyl groups of one taci ligand are deprotonated. Examples: Cr^{3+}, Fe^{3+}, Ga^{3+}.

(5) Sufficiently large ions with a $d^{10}s^2$ electron configuration form trinuclear species by coordinating simultaneously the three sites (ii) of taci. Each of the three ions binds to one amino group and to two deprotonated alkoxo groups. The complex may contain one or two ligand molecules, and the coordination number may vary over a wide range. Additional ligands like water molecules or counterions may interact weakly with the metal. Examples: Pb^{2+}, Bi^{3+}.

Acknowledgment. We thank Beat Müller for measuring the NMR spectra, Martin Colussi for the performance of the thermogravimetric measurements, Rolf Häfliger for recording the mass spectra, and Professor Luigi Mario Venanzi for his careful reading of the manuscript. A part of the synthetic work has been done by Heinz Samaras. This work was supported by the ETH Zürich, Kredite für Unterricht und Forschung.

Supplementary Material Available: Tables SI–SV, listing crystallographic data, anisotropic displacement parameters, positional parameters of hydrogen atoms, bond distances, and bond angles, and Figure S1–S3, showing the thermogravimetric analyses of **3**, **4B**, and **5**, measured and calculated isotope distributions of $[Cd(taci)]^+$, $[Cd(taci) - H]^+$, and $[Cd(taci)_2 - H]^+$, and acidimetric and alkalimetric titration curves of the Cd(II)–taci system (33 pages). Ordering information is given on any current masthead page. A table of calculated and observed structure factors is available from the authors upon request.